OPEN ACCESS Freely available online

PLOS ONE

Structure-Activity Relationships of Novel Salicylaldehyde Isonicotinoyl Hydrazone (SIH) Analogs: Iron Chelation, Anti-Oxidant and Cytotoxic Properties

Eliška Potůčková[1], Kateřina Hrušková[1], Jan Bureš[1], Petra Kovaříková[1], Iva A. Špirková[1], Kateřina Pravdíková[1], Lucie Kolbabová[1], Tereza Hergeselová[1], Pavlína Hašková[1], Hana Jansová[1], Miloslav Macháček[1], Anna Jirkovská[1], Vera Richardson[2], Darius J. R. Lane[2], Danuta S. Kalinowski[2], Des R. Richardson[2], Kateřina Vávrová[1]*, Tomáš Šimůnek[1]*

1 Charles University in Prague, Faculty of Pharmacy in Hradec Králové, Hradec Králové, Czech Republic, **2** Molecular Pharmacology and Pathology Program, Bosch Institute and Department of Pathology, University of Sydney, Sydney, Australia

Abstract

Salicylaldehyde isonicotinoyl hydrazone (SIH) is a lipophilic, tridentate iron chelator with marked anti-oxidant and modest cytotoxic activity against neoplastic cells. However, it has poor stability in an aqueous environment due to the rapid hydrolysis of its hydrazone bond. In this study, we synthesized a series of new SIH analogs (based on previously described aromatic ketones with improved hydrolytic stability). Their structure-activity relationships were assessed with respect to their stability in plasma, iron chelation efficacy, redox effects and cytotoxic activity against MCF-7 breast adenocarcinoma cells. Furthermore, studies assessed the cytotoxicity of these chelators and their ability to afford protection against hydrogen peroxide-induced oxidative injury in H9c2 cardiomyoblasts. The ligands with a reduced hydrazone bond, or the presence of bulky alkyl substituents near the hydrazone bond, showed severely limited biological activity. The introduction of a bromine substituent increased ligand-induced cytotoxicity to both cancer cells and H9c2 cardiomyoblasts. A similar effect was observed when the phenolic ring was exchanged with pyridine (*i.e.*, changing the ligating site from *O*, *N*, *O* to *N*, *N*, *O*), which led to pro-oxidative effects. In contrast, compounds with long, flexible alkyl chains adjacent to the hydrazone bond exhibited specific cytotoxic effects against MCF-7 breast adenocarcinoma cells and low toxicity against H9c2 cardiomyoblasts. Hence, this study highlights important structure-activity relationships and provides insight into the further development of aroylhydrazone iron chelators with more potent and selective anti-neoplastic effects.

Citation: Potůčková E, Hrušková K, Bureš J, Kovaříková P, Špirková IA, et al. (2014) Structure-Activity Relationships of Novel Salicylaldehyde Isonicotinoyl Hydrazone (SIH) Analogs: Iron Chelation, Anti-Oxidant and Cytotoxic Properties. PLoS ONE 9(11): e112059. doi:10.1371/journal.pone.0112059

Editor: Kostas Pantopoulos, Lady Davis Institute for Medical Research/McGill University, Canada

Received June 26, 2014; **Accepted** October 11, 2014; **Published** November 13, 2014

Data Availability: The authors confirm that all data underlying the findings are fully available without restriction. All relevant data are within the paper and its Supporting Information files.

Funding: This study was supported by the Charles University in Prague (www.cuni.cz; projects GAUK 299511, SVV 260065 and 260062), the Czech Science Foundation (www.gacr.cz; grant 13-15008S), and the European Social Fund and the State Budget of the Czech Republic (www.msmt.cz; Operational Program CZ.1.07/2.3.00/30.0061). This work was also funded by a Project Grant from the National Health and Medical Research Council Australia (NHMRC; www.nhmrc.gov.au) to D.R.R. [Grant 632778]; a NHMRC Senior Principal Research Fellowship to D.R.R. [Grant 571123]; and a Cancer Institute New South Wales (cancerinstitute.org.au) Early Career Development Fellowship to D.S.K. [Grant 08/ECF/1–30]. D.J.R.L. thanks the Cancer Institute New South Wales for an Early Career Fellowship [10/ECF/2–18] and the NHMRC of Australia for an Early Career Postdoctoral Fellowship [1013810]. The funders had no role in study design, data collection and analysis, decision to publish, or preparation of the manuscript.

Competing Interests: The authors have declared that no competing interests exist.

* Email: Tomas.Simunek@faf.cuni.cz (TS); Katerina.Vavrova@faf.cuni.cz (KV)

Introduction

Iron is a crucial component of various proteins involved in oxygen transport, cellular respiration, metabolism and division [1,2,3]. The majority of cellular iron acquired by tumor cells is stored in ferritin [4,5], with smaller amounts being utilized for cellular metabolism, such as the synthesis of heme or iron-sulfur clusters [6,7]. Intracellular iron is also found within a poorly defined "labile iron pool" (LIP), in which iron may be in transit between proteins and/or low-molecular weight (M_r) ligands, or specifically transported by putative iron-chaperone proteins, such as poly(rC)-binding proteins 1–4 [8,9].

When intracellular iron is depleted, the synthesis of new iron-dependent proteins and enzymes, and the processes they regulate (*e.g.*, cellular growth and proliferation), can be inhibited [10,11]. On the other hand, when iron is present in excess, iron-mediated oxidative stress can lead to the damage of proteins, lipids and nucleic acids and can be cytotoxic. In fact, "free" or labile redox-active iron can catalyze the Fenton and Haber-Weiss-type reactions that generate highly toxic reactive oxygen species (ROS) [2,4]. Classical iron chelators used in the clinics, such as desferrioxamine (DFO), deferiprone, and deferasirox, sequester iron and are primarily used to manage disorders with increased systemic iron levels, such as that caused by repeated blood transfusions in β-thalassemia major patients [12,13,14]. More recently, iron chelators have been also studied in pathological conditions associated with oxidative stress unrelated to iron-overload diseases [15].

Cancer cells require more iron than their neoplastic counterparts in order to support their increased rates of proliferation [1]. Indeed, iron is a key cofactor of ribonucleotide reductase, an enzyme that catalyzes the rate-limiting step in DNA synthesis [16,17]. Cancer cells up-regulate transferrin (Tf) receptor 1 (TfR1) expression on their surface to increase iron uptake from the iron transport protein, Tf [18,19]. Some cancer cells also express hepcidin, a hormone that induces the internalization of the iron-export protein, ferroportin 1, leading to reduced iron efflux from cells [19,20]. Iron chelators induce iron depletion with subsequent G_1-S cell cycle arrest and apoptosis [21] and they are increasingly studied as potential anti-neoplastic agents, with several in pre-clinical or clinical development [13,22,23].

N′-Salicylaldehyde isonicotinoyl hydrazone (SIH, Fig. 1) is a well-established tridentate iron chelator, which forms 2:1 complexes with both Fe^{3+} and Fe^{2+} ions [24,25]. SIH has been shown to: (***1***) protect various cell types against oxidative stress-inducing agents [15,26,27]; (***2***) prevent the cardiotoxicity of anthracycline-based antineoplastic agents both *in vitro* and *in vivo* [28]; and (***3***) act as a potential radio-protective, anti-viral and anti-cancer agent [29,30,31]. SIH has low *in vitro* and *in vivo* toxicity and good tolerability, even following prolonged administration to animals [32]. Recently, a series of new analogs of SIH were developed that have markedly enhanced hydrolytic stability compared to SIH and retain their ability to protect cells against oxidative injury [33]. In addition, these agents have increased cytotoxic activity compared to SIH [31]. The lead ligands identified in this series included (*E*)-*N′*-[1-(2-hydroxyphenyl)ethylidene]isonicotinoylhydrazide (HAPI; Fig. 1) and (*E*)-*N′*-[1-(2-hydroxyphenyl)propylidene]isonicotinoylhydrazide (HPPI; Fig. 1), which possess either a methyl or ethyl group, respectively, in proximity to the hydrazone bond [31].

To further analyze their structure-activity relationships, in the present study, we designed and synthesized derivatives of SIH, HAPI and HPPI (Fig. 1). The first modification was the reduction of the hydrazone bond leading to *N′*-(2-hydroxybenzyl)isonicotinoylhydrazide (redSIH; Fig. 1), *N′*-[1-(2-hydroxyphenyl)ethyl]isonicotinoylhydrazide (redHAPI; Fig. 1) and *N′*-[1-(2-hydroxyphenyl)propyl]isonicotinoylhydrazide (redHPPI; Fig. 1). These compounds were specifically synthesized to assess the importance of the hydrazone bond for the anti-oxidative and/or cytotoxic activity that has been associated with various aroylhydrazones [34,35,36].

We also studied the effects of bromination at position 5 of the phenolic ring of HAPI and HPPI, leading to (*E*)-*N′*-[1-(5-bromo-2-hydroxyphenyl)ethylidene]isonicotinoylhydrazide (BHAPI; Fig. 1) and (*E*)-*N′*-[1-(5-bromo-2-hydroxyphenyl)propylidene]isonicotinoylhydrazide (BHPPI; Fig. 1), respectively. The effect of halogenation was examined since a previous study demonstrated the high cytotoxic activity of a chloro-substituted ligand [31]. An analog, in which the phenolic ring of HAPI was exchanged for pyridine, was also prepared ((*E*)-*N′*-[1-(pyridin-2-yl)ethylidene]isonicotinoylhydrazide; 2API; Fig. 1) to assess the effects on its properties of changing the ligating groups from *O*, *N*, *O* to *N*, *N*, *O*. The chelation properties of 2API would be different from those of SIH because the pyridine nitrogen in 2API is a softer base relative to the hard phenolic oxygen in SIH. Considering this, 2API would be able to bind both Fe^{3+} and Fe^{2+} ions, while SIH and its analogs prefer Fe^{3+}. Thus, although 2API does not belong to the same ligand category as SIH, we aimed to explore its properties because 2API is a methyl analog of 2-pyridylcarboxaldehyde isonicotinoyl hydrazone (PCIH), which was developed for the treatment of iron overload [37,38].

An analog of HAPI with a 2C side chain as a part of an indane ring was also synthesized, leading to (*E*)-*N′*-(7-hydroxy-2,3-dihydro-1*H*-inden-1-ylidene)isonicotinoylhydrazide (7HII; Fig. 1). Analogs of HAPI and HPPI with varying alkyl groups adjacent to the hydrazone bond were also prepared, including derivatives containing an isopropyl substituent ((*E*)-*N′*-(1-(2-hydroxyphenyl)-2-methylpropylidene)isonicotinoylhydrazide; H16; Fig. 1), propyl substituent ((*E*)-*N′*-[1-(2-hydroxyphenyl)butylidene]isonicotinoylhydrazide; H17; Fig. 1), isobutyl substituent ((*E*)-*N′*-(1-(2-hydroxyphenyl)-3-methylbutylidene)isonicotinoylhydrazide; H18; Fig. 1), or cyclohexyl ring ((*E*)-*N′*-[cyclohexyl(2-hydroxyphenyl)-methylene]isonicotinoylhydrazide; H28; Fig. 1).

To characterize these new ligands, we examined their: (***1***) stability against hydrolysis in plasma; (***2***) iron chelation and redox properties; (***3***) protective potential against oxidative injury induced by exposure of H9c2 rat embryonic cardiomyoblast cells to hydrogen peroxide (H_2O_2); (***4***) cytotoxic activity using neoplastic MCF-7 breast adenocarcinoma cells; and (***5***) selectivity by comparing their cytotoxic effects to the non-tumorigenic, cardiomyoblast cell line, H9c2. These studies are important for dissecting structure-activity relationships that are essential for the development of more effective ligands.

Materials and Methods

1 Syntheses of chelators

All chemicals were purchased from Sigma-Aldrich (St. Louis, MO, USA). Thin layer chromatography was performed on TLC sheets (silica gel 60 F254) from Merck (Darmstadt, Germany). Microwave reactions were conducted in a Milestone Micro-SYNTH Ethos 1600 URM apparatus. Melting points were measured on a Kofler apparatus and are uncorrected. All products were characterized by NMR (Varian Mercury Vx BB 300 or VNMR S500 NMR spectrometers). Chemical shifts were reported as δ values in parts per million (ppm) and were indirectly referenced to tetramethylsilane (TMS) *via* the solvent signal. All assignments were based on 1D experiments. Elemental analysis was measured on a CHNS-OCE FISONS EA 1110 apparatus.

***N′*-Salicylaldehyde isonicotinoyl hydrazone (SIH).** SIH was synthesized as described previously [39]. Yellow crystalline solid. mp 232–234°C. ^{1}H NMR (300 MHz, DMSO-d_6): δ 12.29 (s, 1H, OH), 11.02 (s, 1H, NH), 8.80 (d, J = 4.4 Hz, 2H, Py), 8.68 (s, 1H, CH), 7.85 (d, J = 4.4 Hz, 2H, Py), 7.61 (dd, J = 7.7, 1.5 Hz, 1H, Ph), 7.36–7.28 (m, 1H, Ph), 6.95–6.88 (m, 2H, Ph). ^{13}C NMR (75 MHz, DMSO-d_6): δ 163.1, 157.5, 150.4, 148.9, 141.2, 131.7, 129.2, 121.5, 119.5, 116.4.

***N′*-(2-hydroxybenzyl)isonicotinoylhydrazide (redSIH).** SIH (0.69 g, 2.8 mmol) was dissolved in 96% (v/v) ethanol (50 mL) and $NaBH_3CN$ (0.36 g, 5.7 mmol) was added. The reaction mixture was adjusted to a pH of 3-5 using a 10% (v/v) solution of HCl in methanol. The reaction mixture was stirred at room temperature (RT) overnight and was then neutralized with a solution of sodium bicarbonate to pH 7. The reaction mixture was evaporated to dryness and was then partitioned against water and EtOAc. The combined organic layers were dried with anhydrous Na_2SO_4 and evaporated under reduced pressure. The product was purified with column chromatography on silica using hexane/EtOAc (1:1) as a mobile phase. The product was isolated as a white crystalline solid. Yield 0.17 g (24%). mp 143–146°C. ^{1}H NMR (300 MHz, DMSO-d_6): δ 10.43 (s, 1H, OH), 9.61 (s, 1H, NH), 8.70 (d, J = 5.1 Hz, 2H, Py), 7.74–7.65 (m, 2H, Py), 7.20 (dd, J = 7.5, 1.7 Hz, 1H, Ph), 7.12–7.02 (m, 1H, Ph), 6.84–6.67 (m, 2H, Ph), 5.65 (s, 1H, NH), 3.95 (d, J = 6.0 Hz, 2H, CH_2). ^{13}C NMR (75 MHz, DMSO-d_6): δ 163.5, 156.1, 150.4, 140.3, 130.1, 128.5, 124.1, 121.3, 118.9, 115.3, 50.7. Anal. Calcd. for $C_{13}H_{13}N_3O_2$: C, 64.19; H, 5.39; N, 17.27; Found: C, 64.50; H, 5.26; N, 17.56.

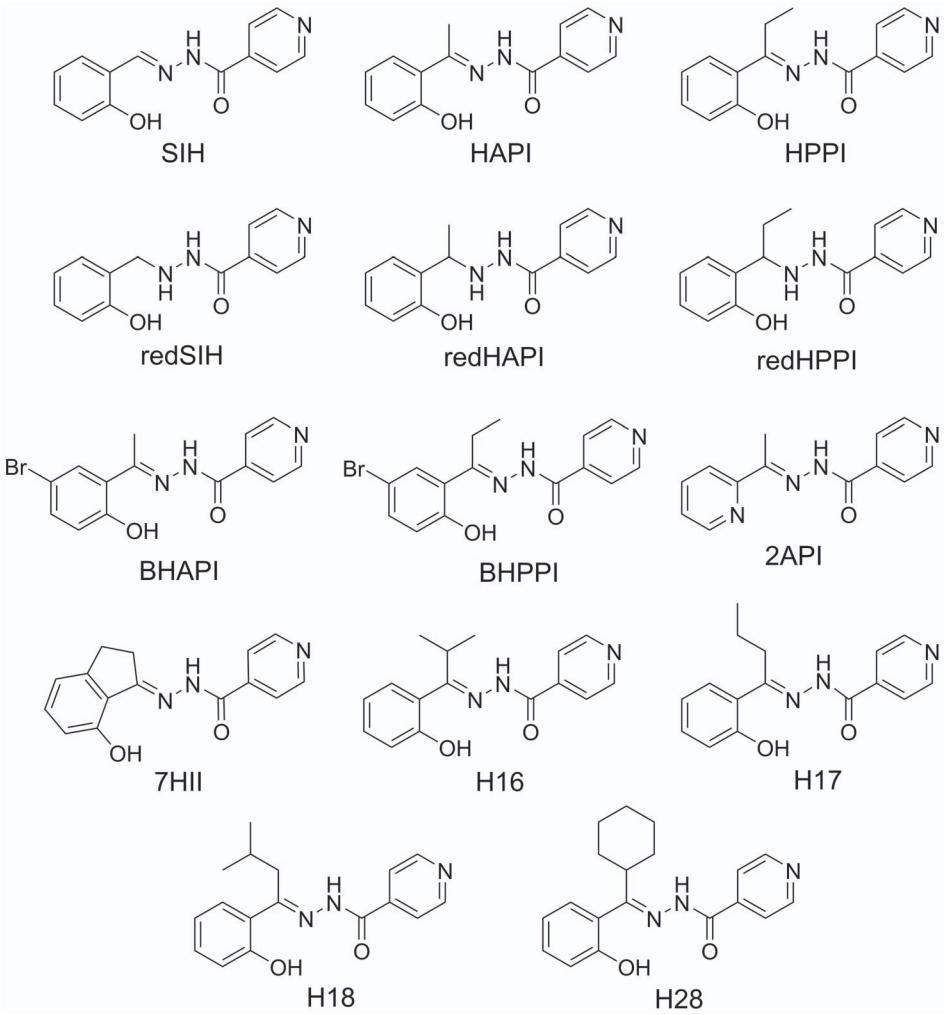

Figure 1. Line drawings of the chemical structures of the iron chelators, SIH, HAPI and HPPI, and their novel analogs.
doi:10.1371/journal.pone.0112059.g001

***N′*-[1-(2-Hydroxyphenyl)ethyl]isonicotinoylhydrazide (redHAPI).** The initial chelator, (*E*)-*N′*-[1-(2-hydroxyphenyl)ethylidene]isonicotinoylhydrazide (HAPI), was synthesized as described previously [33]. The reduced analog, redHAPI, was prepared from HAPI as described above for redSIH. The product was isolated as a yellow solid. Yield 0.18 g (26%). mp 131–134°C. ^{1}H NMR (500 MHz, DMSO-d_6): δ 10.29 (s, 1H, OH), 9.63 (s, 1H, NH), 8.70 (m, 2H, Py), 7.68 (d, J = 4.8 Hz, 2H, Py), 7.29 (dd, J = 7.8, 1.7 Hz, 1H, Ph), 7.11–7.00 (m, 1H, Ph), 6.82–6.69 (m, 2H, Ph), 5.57 (s, 1H, NH), 4.53–4.27 (m, 1H, CH), 1.28 (d, J = 6.6 Hz, 3H, CH_3). ^{13}C NMR (125 MHz, DMSO-d_6): δ 164.1, 155.4, 150.4, 140.3, 129.1, 127.9, 127.3, 124.9, 119.1, 115.6, 54.3, 19.7. Anal. Calcd. for $C_{14}H_{15}N_3O_2$: C, 65.36; H, 5.88; N, 16.33; Found: C, 64.98; H, 6.04; N, 16.53.

***N′*-[1-(2-Hydroxyphenyl)propyl]isonicotinoylhydrazide (redHPPI).** The initial chelator, (*E*)-*N′*-[1-(2-hydroxyphenyl)propylidene]isonicotinoylhydrazide (HPPI), was synthesized as described previously [33]. The reduced analog, redHPPI was prepared from HPPI as described above for redSIH. The product was obtained as a yellow solid. Yield 0.29 g (42%). mp 115–118°C. ^{1}H NMR (500 MHz, DMSO-d_6): δ 10.21 (s, 1H, NH), 9.58 (s, 1H, NH), 8.90–8.55 (m, 2H, Py), 7.83–7.55 (m, 2H, Py), 7.27 (dd, J = 7.6, 1.7 Hz, 1H, Ph), 7.10 (m, 1H, Ph), 6.82–6.68 (m, 2H, Py), 5.62 (s, 1H, OH), 4.21 (t, J = 6.6 Hz, 1H, CH), 1.81–1.60 (m, 2H, CH_2), 1.14 (t, J = 7.6 Hz, 3H, CH_3). ^{13}C NMR (125 MHz, DMSO-d_6): δ 163.8, 155.8, 150.3, 140.3, 128.4, 127.8, 124.9, 118.9, 115.6, 60.6, 26.0, 10.7. Anal. Calcd. for $C_{15}H_{17}N_3O_2$: C, 66.40; H, 6.32; N, 15.49; Found: C, 66.42; H, 6.45; N, 15.55.

(*E*)-*N′*-[1-(5-Bromo-2-hydroxyphenyl)ethylidene]isonicotinoylhydrazide (BHAPI). Isoniazid (0.21 g, 1.5 mmol), 5-bromo-2-hydroxyacetophenone (0.32 g, 1.5 mmol) and acetic acid (0.25 mL) were dissolved in methanol (5 mL) and stirred for 2 h under reflux in the microwave reactor described above. The reaction mixture was then cooled to 4°C and the resulting precipitate was collected by filtration, washed with water and methanol and dried over P_2O_5 to give 0.2 g (39%) of the product as a yellow crystalline solid. mp 225–227°C. ^{1}H NMR (500 MHz, DMSO-d_6): δ 13.27 (s, 1H, OH), 11.66 (s, 1H, NH), 8.82–8.76 (m, 2H, Py), 7.86–7.79 (m, 2H, Py), 7.76 (d, J = 2.3 Hz, 1H, Ph), 7.45 (dd, J = 8.8, 2.2 Hz, 1H, Ph), 6.90 (d, J = 8.7 Hz, 1H, Ph), 2.49 (s, 3H, CH_3). ^{13}C NMR (125 MHz, DMSO-d_6): δ 163.3, 158.1, 158.0, 150.4, 140.1, 134.1, 131.0, 122.2, 121.5, 119.8, 109.9, 14.7. Anal. Calcd. for $C_{14}H_{14}BrN_3O_2$: C, 50.32; H, 3.62; N, 12.57; Found: C 50.71; H, 3.99; N, 12.88.

(*E*)-*N′*-[1-(5-Bromo-2-hydroxyphenyl)propylidene]isonicotinoylhydrazide (BHPPI). Isoniazid (0.2 g, 1.4 mmol), 5-bromo-2-hydroxypropiophenone (0.33 g, 1.4 mmol) and acetic acid (0.25 mL) were dissolved in methanol (5 mL) and stirred overnight

under reflux. After cooling the reaction mixture to 4°C, the resulting precipitate was collected by filtration, washed with water and methanol and dried over P_2O_5 to give 0.32 g (64%) of the product as a yellow crystalline solid. mp 239–242°C. ^{1}H NMR (500 MHz, DMSO-d_6): δ 13.33 (s, 1H, OH), 11.69 (s, 1H, NH), 8.79 (d, J = 5.0 Hz, 2H, Py), 7.86–7.81 (m, 3H, Py, Ph), 7.45 (dd, J = 8.8, 2.4 Hz, 1H, Ph), 6.92 (d, J = 8.7 Hz, 1H, Ph), 3.01 (q, J = 7.6 Hz, 2H, CH_2), 1.09 (t, J = 7.0 Hz, 3H, CH_3). ^{13}C NMR (125 MHz, DMSO-d_6): δ 163.8, 161.2, 158.5, 150.3, 140.3, 134.0, 130.5, 122.4, 120.2, 120.1, 109.9, 19.7, 11.4. Anal. Calcd. for: $C_{15}H_{16}BrN_3O_2$: C, 51.74; H, 4.05; N, 12.07; Found: C, 51.41; H, 4.26; N, 11.74.

(*E*)-*N*′-[1-(Pyridin-2-yl)ethylidene]isonicotinoylhydrazide (2API). Isoniazid (0.57 g, 4.1 mmol), 2-acetylpyridine (0.5 g, 3.4 mmol) and acetic acid (0.25 mL) were dissolved in methanol (10 mL) and stirred overnight under reflux. After cooling the reaction mixture to 4°C, the resulting precipitate was collected by filtration, washed with water and methanol and dried over P_2O_5 to give 0.37 g (37%) of the product as a white crystalline solid. mp 166°C. ^{1}H NMR (500 MHz, DMSO-d_6): δ 11.10 (s, 1H, NH), 8.77 (d, J = 5.1 Hz, 2H, Py), 8.62 (d, J = 5.3 Hz, 1H, Py'), 8.12 (d, J = 8.2 Hz, 1H, Py'), 7.90–7.40 (m, 1H, Py'), 7.83–7.77 (m, 2H, Py), 7.47–7.40 (m, 1H, Py'), 2.47 (s, 3H, CH_3). ^{13}C NMR (125 MHz, DMSO-d_6): δ 163.0, 155.1, 150.3, 149.7, 141.2, 136.9, 124.7, 122.2, 121.2, 13.1. Anal. Calcd. for $C_{13}H_{12}N_4O$: C, 64.99; H, 5.03; N, 23.32; Found: C, 65.33; H, 5.31; N, 23.43.

(*E*)-*N*′-(7-Hydroxy-2,3-dihydro-1*H*-inden-1-ylidene)isonicotinoylhydrazide (7HII). Isoniazid (0.46 g, 3.4 mmol), 7-hydroxy-2,3-dihydro-1*H*-inden-1-one (0.5 g, 3.4 mmol) and acetic acid (0.25 mL) were dissolved in methanol (10 mL) and stirred overnight under reflux. After cooling the reaction mixture to 4°C, the resulting precipitate was collected by filtration and washed with water and methanol. The solid was suspended in toluene and was stirred for 30 min. This solution was filtered to obtain 0.37 g (66%) of the product as a yellow crystalline solid. mp 232–236°C. ^{1}H NMR (500 MHz, DMSO-d_6): δ 11.30 (s, 1H, NH), 10.15 (s, 1H, OH), 8.80–8.70 (m, 2H, Py), 7.84–7.74 (m, 2H, Py), 7.30 (dd, J = 7.8, 1.3 Hz, 1H, Ph), 6.89 (d, J = 7.4 Hz, 1H, Ph), 6.75 (d, J = 8.1 Hz, 1H, Ph), 3.13–3.00 (m, 4H, 2xCH_2). ^{13}C NMR (125 MHz, DMSO-d_6): δ 167.9, 162.5, 155.5, 150.3, 150.0, 140.8, 133.1, 122.6, 122.1, 116.6, 113.0, 28.7, 28.1. Anal. Calcd. for $C_{15}H_{13}N_3O_2$: C, 67.40; H, 4.90; N, 15.72; Found: C, 67.02; H, 5.13; N, 15.87.

(*E*)-*N*′-(1-(2-Hydroxyphenyl)-2-methylpropylidene)isonicotinoylhydrazide (H16). To prepare H16, 1-(2-hydroxyphenyl)-2-methylpropan-1-one was first synthesized: 2-hydroxybenzonitrile (0.36 g, 3 mmol) was dissolved in dry THF (5 mL) and a solution of isopropylmagnesium chloride in THF (2 M, 6.1 mL, 1.2 mmol) was added and the reaction mixture refluxed for 2 h. The reaction mixture was cooled in an ice bath, 10 mL of cold water was carefully added and cold concentrated H_2SO_4 added dropwise to obtain an acidic pH. The reaction mixture was then heated for 1 h at 80°C and, after cooling to RT, it was extracted twice with diethyl ether. The combined organic layer was dried with anhydrous Na_2SO_4 and evaporated under reduced pressure. The product was purified by column chromatography on silica using hexane/EtOAc (40:1) as the mobile phase. The product was obtained as a yellow oil. Yield 0.45 g (91%). ^{1}H NMR (300 MHz, $CDCl_3$): δ 12.52 (s, 1H, OH), 7.79 (dd, J = 8.1, 1.6 Hz, 1H, Ph), 7.53–7.40 (m, 1H, Ph), 7.04–6.84 (m, 2H, Ph), 3.70–3.54 (m, 1H, CH), 1.43–1.14 (m, 6H, 2xCH_3). ^{13}C NMR (75 MHz, $CDCl_3$): δ 210.9, 163.1, 136.2, 129.8, 118.8, 118.7, 118.1, 34.9, 29.7, 19.3.

1-(2-Hydroxyphenyl)-2-methylpropan-1-one (0.29 g, 1.8 mmol), isoniazid (0.24 g, 1.8 mmol) and acetic acid (0.25 mL) were dissolved in methanol (5 mL) and heated at 110°C in an autoclave for 48 h. After cooling to RT, water was added dropwise until the solution turned cloudy and the mixture was left to crystallize at 4°C for 24 h. The precipitate was collected by filtration, washed with water and methanol and dried over P_2O_5 to yield 0.07 g (14%) of H16 as a white crystalline solid. mp 228–235°C. ^{1}H NMR (300 MHz, DMSO-d_6): δ 10.08 (s, 1H, NH), 8.66 (m, 2H, Py), 7.66 (m, 2H, Py), 7.43 (d, J = 7.7 Hz, 1H, Ph), 7.35–7.22 (m, 1H, Ph), 7.13 (d, J = 7.7 Hz, 1H, Ph), 7.03–6.79 (m, 1H, Ph), 3.07–2.80 (m, 1H, CH), 1.42–0.78 (m, 6H, 2xCH_3). ^{13}C NMR (75 MHz, DMSO-d_6): δ 163.7, 163.3, 153.9, 150.4, 141.4, 130.9, 128.8, 121.2, 120.7, 119.7, 116.2, 35.9, 20.1. Anal. Calcd. for $C_{16}H_{17}N_3O_2$: C, 67.83; H, 6.05; N, 14.83; Found: C, 67.44; H, 6.37; N, 14.83.

(*E*)-*N*′-[1-(2-Hydroxyphenyl)butylidene]isonicotinoylhydrazide (H17). To prepare H17, 1-(2-hydroxyphenyl)butan-1-one was first synthesized: Magnesium (0.3 g, 12 mmol) was suspended in dry THF (5 mL), and propylbromide (1.5 g, 12 mmol) was added dropwise and the mixture refluxed for 2 h until the magnesium dissolved. After cooling the reaction mixture to RT, 2-hydroxybenzonitrile (0.36 g, 3 mmol) dissolved in dry THF (5 mL) was added dropwise and the reaction refluxed for 2 h. The reaction mixture was cooled in an ice bath, 10 mL of cold water was carefully added and cold concentrated H_2SO_4 added dropwise to obtain an acidic pH. The reaction mixture was then heated for 1 h at 80°C and, after cooling to RT, it was extracted twice with diethyl ether. The combined organic layer was dried with anhydrous Na_2SO_4 and evaporated under reduced pressure. The product was purified by column chromatography on silica (gradient; hexane to hexane/EtOAc 40:1). The product was obtained as a yellow oil. Yield: 0.41 g (82%). ^{1}H NMR (300 MHz, $CDCl_3$): δ 7.90–7.67 (m, 1H, Ph), 7.57–7.36 (m, 1H, Ph), 7.05–6.76 (m, 2H, Ph), 2.79 (t, J = 7.3 Hz, 2H, CH_2), 1.69–1.43 (m, 2H, CH_2), 1.03 (t, J = 7.4 Hz, 3H, CH_3). ^{13}C NMR (75 MHz, $CDCl_3$): δ 206.8, 162.5, 136.2, 130.0, 119.4, 118.8, 118.5, 40.2, 17.9, 13.8.

1-(2-Hydroxyphenyl)-butan-1-one (0.39 g, 2.4 mmol), isoniazid (0.33 g, 2.4 mmol) and acetic acid (0.25 mL) were dissolved in methanol (5 mL) and heated at 110°C in an autoclave for 72 h. After cooling to RT, water was added dropwise until the solution turned cloudy and the mixture was left to crystallize at 4°C for 24 h. The precipitate was collected by filtration, washed with water and methanol and dried over P_2O_5 to yield 0.08 g (12%) of the product as a white crystalline solid. mp 189–192°C. ^{1}H NMR (500 MHz, DMSO-d_6): δ 8.79 (d, J = 5.3, 2H, Py), 7.89–7.72 (m, 2H, Py), 7.63 (dd, J = 8.1, 1.6 Hz, 1H, Ph), 7.30 (ddd, J = 8.4, 7.1, 1.5 Hz, 1H, Ph), 7.00–6.79 (m, 2H, Ph), 3.06–2.86 (m, 2H, CH_2), 1.73–1.44 (m, 2H, CH_2), 0.99 (t, J = 7.3 Hz, 3H, CH_3). ^{13}C NMR (125 MHz, DMSO-d_6): δ 163.6, 161.7, 159.4, 150.3, 140.5, 131.6, 128.7, 122.3, 118.8, 118.3, 117.8, 27.9, 20.3, 13.9. Anal. Calcd. for $C_{16}H_{17}N_3O_2$: C, 67.83; H, 6.05; N, 14.83; Found: C, 67.42; H, 6.41; N, 14.55.

(*E*)-*N*′-(1-(2-Hydroxyphenyl)-3-methylbutylidene)isonicotinoylhydrazide (H18). To prepare H18, 1-(2-hydroxyphenyl)-3-methylbutan-1-one was first synthesized: Magnesium (0.41 g, 16.9 mmol) was suspended in dry THF (5 mL), and isobutylbromide (2.31 g, 16.7 mmol) was added dropwise and the mixture refluxed for 2 h until the magnesium dissolved. After cooling the reaction mixture to RT, 2-hydroxybenzonitrile (0.33 g, 2.8 mmol) dissolved in dry THF (5 mL) was added dropwise and the reaction refluxed for 2 h. The reaction mixture was cooled in an ice bath, 10 mL of cold water was carefully added and cold concentrated H_2SO_4 added dropwise to obtain an acidic pH. The reaction mixture was then heated for 1 h at 80°C and, after cooling to RT, it was extracted twice with diethyl

ether. The combined organic layer was dried with anhydrous Na_2SO_4 and evaporated under reduced pressure. The product was purified by column chromatography on silica using hexane/EtOAc (40:1) as the mobile phase. The product was a yellow oil. Yield 0.45 g (91%). ^{1}H NMR (300 MHz, $CDCl_3$): δ 12.48 (s, 1H, OH), 7.89–7.63 (m, 1H, Ph), 7.59–7.40 (m, 1H, Ph), 7.08–6.83 (m, 2H, Ph), 2.92–2.74 (m, 2H, CH_2), 2.38–2.22 (m, 1H, CH), 1.13–0.94 (m, 6H, 2xCH_3). ^{13}C NMR (75 MHz, $CDCl_3$): δ 206.7, 162.6, 136.2, 130.1, 119.6, 118.8, 118.5, 47.1, 25.5, 22.7.

1-(2-Hydroxyphenyl)-3-methylbutan-1-one (0.2 g, 1.1 mmol), isoniazid (0.12 g, 1.1 mmol) and acetic acid (0.25 mL) were dissolved in methanol (5 mL) and heated at 110°C in an autoclave for 72 h. After cooling to RT, water was added dropwise until the solution turned cloudy and the mixture was left to crystallize at 4°C. The precipitate was then collected by filtration, washed with water and methanol and dried over P_2O_5. The overall yield of the white crystalline product was 0.06 g (19%). mp 144–146°C. ^{1}H NMR (500 MHz, DMSO-d_6): δ 13.27 (s, 1H, OH), 11.61 (s, 1H, NH), 8.82–8.77 (m, 2H, Py), 7.81–7.73 (m, 2H, Py), 7.65 (dd, J = 8.0, 1.7 Hz, 1H, Ph), 7.42–7.19 (m, 1H, Ph), 6.97–6.86 (m, 2H, Ph), 2.99 (d, J = 7.4 Hz, 2H, CH_2), 2.02–1.93 (m, 1H, CH), 0.95 (d, J = 6.6 Hz, 6H, 2xCH_3). ^{13}C NMR (125 MHz, DMSO-d_6): δ 163.3, 161.5, 159.2, 150.4, 140.4, 131.6, 129.0, 122.2, 118.7, 117.8, 34.3, 27.6, 22.2. Anal. Calcd. for $C_{17}H_{19}N_3O_2$: C, 68.67; H, 6.44; N, 14.13; Found: C, 68.28; H, 6.69; N, 13.85.

(*E*)-*N*′-[Cyclohexyl(2-hydroxyphenyl)methylene]isonicotinoylhydrazide (H28). To prepare H28, cyclohexyl(2-hydroxyphenyl)methanone was synthesized: Magnesium (0.36 g, 15 mmol) was suspended in dry THF (5 mL) and cyclohexylbromide (2.4 g, 15 mmol) was added dropwise. This reaction mixture was refluxed for 2 h until the magnesium dissolved. After cooling the reaction mixture to RT, 2-hydroxybenzonitrile (0.29 g, 2.4 mmol) dissolved in dry THF (5 mL) was added dropwise and the reaction refluxed for 3 h. The reaction mixture was cooled in an ice bath, 10 mL of cold water was added carefully and then cold concentrated H_2SO_4 was added dropwise to obtain an acidic pH. The reaction mixture was then heated overnight at 80°C and, after cooling to RT, it was extracted twice with diethyl ether. The combined organic layer was dried with anhydrous Na_2SO_4 and evaporated under reduced pressure. The product was purified by column chromatography on silica (gradient; hexane to hexane/EtOAc 40:1). The product was obtained as a yellow oil. Yield 0.49 g (97%). ^{1}H NMR (300 MHz, $CDCl_3$) δ 12.58 (s, 1H, OH), 7.88–7.69 (m, 1H, Ph), 7.55–7.32 (m, 1H, Ph), 7.07–6.95 (m, 2H, Ph), 3.43–3.12 (m, 1H, Cy), 2.03–1.06 (m, 10H, Cy). ^{13}C NMR (75 MHz, $CDCl_3$): δ 210.1, 163.1, 136.1, 129.8, 118.7, 118.7, 118.2, 45.2, 29.5, 25.8, 25.7.

Cyclohexyl(2-hydroxyphenyl)methanone (0.19 g, 0.93 mmol), isoniazid (0.13 g, 0.93 mmol) and acetic acid (0.20 mL) were dissolved in methanol (5 mL) and heated at 110°C in an autoclave for 4 days. After cooling to RT, water was added dropwise until the solution turned cloudy and the mixture was left to crystallize at 4°C for 24 h. The precipitate was collected by filtration, washed with methanol and dried over P_2O_5 to give 0.046 g (15%) of the product as a white solid. mp 251–253°C. ^{1}H NMR (300 MHz, DMSO-d_6): δ 9.27 (s, 1H, NH), 8.70–8.63 (m, 2H, Py), 7.86–7.70 (m, 2H, Py), 7.51–7.34 (m, 1H, Ph), 7.33–7.19 (m, 1H, Ph), 7.17–7.02 (m, 1H, Ph), 7.02–6.78 (m, 1H, Ph), 2.69–2.34 (m, 1H, Cy), 1.92–1.00 (m, 10H, Cy). ^{13}C NMR (75 MHz, DMSO-d_6): δ 163.0, 161.3, 150.4, 141.4, 130.8, 128.8, 121.2, 120.8, 119.7, 116.2, 30.3, 29.9, 26.0, 25.8. Anal. Calcd. for $C_{19}H_{21}N_3O_2$: C, 70.57; H, 6.55; N, 12.99; Found: C, 70.36; H, 6.91; N, 13.03.

2 Stability study

2.1 HPLC instrument and chromatographic conditions. HPLC analyses were performed on a Prominence LC 20A chromatographic system (Shimadzu, Kyoto, Japan) consisting of a DGU-20A3 degasser, two LC-20AD pumps, SIL-20AC autosampler, a CTO-20AC column oven, SPD-20AC detector and a CBM-20AC communication module. The data were processed by LC solution software, version 1.21 SP1 (Shimadzu).

Analysis of new chelators were performed using an Ascentis C18 chromatographic column (10×3 mm, 3 μm) protected with a guard column with the same sorbent (Sigma-Aldrich). The mobile phase was composed of 1 mM EDTA in 5 mM phosphate buffer and methanol in different ratios (Table 1). The column oven was set at 25°C and the autosampler at 5°C. A flow rate of 0.3 mL/min and injection volume of 20 μL were used. Chromatographic conditions for the determination of each chelator are given in Table 1.

The linearity, precision and accuracy of the methods were examined by the analysis of plasma samples spiked with different amounts of the chelators. Selectivity was confirmed by an analysis of blank plasma samples. All evaluated parameters reached acceptable values [40]. SIH was analyzed using a previously developed and validated method [41].

2.2 Assessment of the chelator stabilities in rabbit plasma. The drug-free plasma samples were spiked with a standard solution of each chelator (1 mg/mL in DMSO) to obtain a concentration of 100 μM. The final chelator-spiked plasma samples were maintained at 37°C and stirred at 300 rpm. Samples of the studied chelators in plasma (50 μL) were transferred into Eppendorf tubes on ice at time intervals of t = 0, 60, 120, 180, 240, 300, 360, 420, 480, 540 and 600 min from the beginning of the experiment. After this procedure, internal standards (IS) were added to the samples and then the plasma proteins were precipitated by adding methanol (200 μL). Precipitates were separated by centrifugation (10,000 rpm/10 min) and the clear supernatant was injected onto the column. In the case of redSIH, redHAPI, redHPPI and 2API, the supernatant was diluted using deionized water at a 1:1 ratio to obtain acceptable peak shapes.

3 Biological studies

3.1 Chemicals. Constituents for various buffers as well as other chemicals (*e.g.*, various iron salts) were purchased from Sigma-Aldrich, Merck or Penta (Prague, Czech Republic) and were of the highest pharmaceutical or analytical grade available.

3.2 Cell cultures. The MCF-7 human breast adenocarcinoma cell line was purchased from the European Collection of Cell Cultures (ECACC; Salisbury, UK), and the H9c2 cardiomyoblast cell line, derived from embryonic rat heart tissue, was obtained from the American Type Culture Collection (ATCC; Manassas, VA, USA). Cells were cultured in Dulbecco's modified Eagle's medium (DMEM; Lonza, Verviers, Belgium) with (H9c2) or without (MCF-7) phenol red and were supplemented with 10% (v/v) heat-inactivated fetal bovine serum (FBS; Lonza), 1% penicillin/streptomycin solution (Lonza) and 10 mM HEPES buffer (pH 7.0–7.6; Sigma-Aldrich). Both cell lines were cultured in 75 cm^2 tissue culture flasks (TPP, Trasadingen, Switzerland) at 37°C in a humidified atmosphere of 5% CO_2. Sub-confluent cells (70–80% confluency) were sub-cultured every 3-4 days.

3.3 Determination of iron chelating efficacy in solution. To assess the iron chelation efficiency of the newly synthesized agents in solution, their ability to remove iron from the iron-calcein complex was examined [42]. Calcein is a fluorescent probe that readily forms iron complexes [42]. Upon formation of

Table 1. Chromatographic conditions used for the determination of the stability of the new chelators in rabbit plasma.

Chelator	Mobile phase ratio (v/v)	UV (nm)	IS
redSIH	40:60	254	redHAPI
redHAPI	40:60	254	7HII
redHPPI	40:60	254	7HII
BHAPI	30:70	254	o-108
BHPPI	30:70	254	7HII
2API	40:60	297	SIH
7HII	30:70	297	BHPPI
H16	40:60	254	o-108
H17	30:70	297	H28
H18	30:70	297	H28
H28	30:70	254	H18

doi:10.1371/journal.pone.0112059.t001

the iron-calcein complex, the fluorescence of calcein is quenched. The addition of another chelating agent to the iron-calcein complex leads to the removal of iron from this complex, resulting in the formation of the new iron-chelator complex. The removal of iron from the iron-calcein complex is accompanied by an increase in fluorescence intensity (*i.e.*, de-quenching), due to the formation of free calcein. Thus, the measurement of calcein fluorescence intensity was used to examine the iron chelation efficacy of the novel chelators [42].

A complex of calcein (free acid, 20 nM; Molecular Probes, Eugene, OR, USA) with iron derived from ferrous ammonium sulfate (200 nM) was prepared in HBS buffer (150 mM NaCl, 40 mM HEPES, pH 7.2). Calcein and ferrous ammonium sulfate were continuously stirred for 45 min in the dark, after which $>$ 90% of the fluorescence was quenched. Then, 995 μL of the complex was pipetted into a stirred cuvette and baseline measurements were acquired. After 100 s, 5 μL of the novel chelator solution was added, yielding a final chelator concentration of 5 μM. Fluorescence intensity change was measured as a function of time at RT using a Perkin Elmer LS50B fluorimeter (Perkin Elmer, Waltham, MA, USA) at $\lambda_{ex} = 486$ nm and $\lambda_{em} = 517$ nm for 350 s. The iron chelation efficiency in solution was expressed as a percentage of the efficiency of the reference chelator, SIH (100%).

3.4 Calcein-AM assay to assess the cell membrane permeability and access to the labile iron pool. These experiments were performed according to Glickstein *et al.* [43] with slight modifications. MCF-7 cells were seeded in 96-well plates (10,000 cells per well). Cells were loaded with iron using the iron donor, ferric ammonium citrate (530 μg/mL), 24 h prior to the experiment, and the cells then washed. To prevent potential interference (especially with regard to various trace elements), the medium was replaced with the ADS buffer (prepared using Millipore water (18.2 MΩ/cm) supplemented with 116 mM NaCl, 5.3 mM KCl, 1 mM $CaCl_2$, 1.2 mM $MgSO_4$, 1.13 mM NaH_2PO_4, 5 mM D-glucose, and 20 mM HEPES, pH 7.4). Cells were then loaded with the membrane-permeant, calcein green acetoxymethyl ester (calcein-AM; 2 μM; Molecular Probes) for 30 min/37°C, and then washed. Cellular esterases cleave the acetoxymethyl groups to form the cell membrane-impermeant compound, calcein green, whose fluorescence is quenched upon binding iron. Intracellular fluorescence ($\lambda_{ex} = 488$ nm; $\lambda_{em} = 530$ nm) was then measured as a function of time (1 min before and 10 min after the addition of chelator) at 37°C using a Tecan Infinite 200 M plate reader (Tecan Group, Männedorf, Switzerland). The iron chelation efficiency in cells was expressed as a percentage of the efficiency of the reference chelator, SIH (100%).

3.5 Preparation of $^{59}Fe_2$-transferrin. Human Tf (Sigma-Aldrich) was labeled with Fe or ^{59}Fe (PerkinElmer) to produce Fe_2-Tf or $^{59}Fe_2$-Tf, respectively, with a final specific activity of 500 pCi/pmol Fe, as previously described [34,44]. Unbound ^{59}Fe was removed by exhaustive vacuum dialysis against an excess of 0.15 M NaCl buffered at pH 7.4 with 1.4% (w/v) $NaHCO_3$ by standard methods [34,44].

3.6 The effect of chelators on mobilizing cellular ^{59}Fe. The ability of the novel ligands to mobilize ^{59}Fe from MCF-7 cells was examined by conducting ^{59}Fe efflux experiments using established techniques [34,45]. In brief, after pre-labeling cells with $^{59}Fe_2$-Tf (0.75 μM) for 3 h/37°C, the cell cultures were washed four times with ice-cold PBS and then subsequently incubated with each chelator (25 μM) for 3 h/37°C. The overlying media containing released ^{59}Fe was then carefully separated from the cells using a Pasteur pipette. Radioactivity was measured in both the cell pellet and supernatant using a γ-scintillation counter (Wallac Wizard 3, Turku, Finland).

3.7 The effect of the chelators on the prevention of cellular ^{59}Fe uptake from ^{59}Fe2-Tf. The ability of the chelators to prevent cellular ^{59}Fe uptake from $^{59}Fe_2$-Tf was examined using standard methods [46,47]. In brief, MCF-7 cells were incubated with $^{59}Fe_2$-Tf (0.75 μM) for 3 h/37°C in the presence of the assessed chelators (25 μM). The cells were then washed four times with ice-cold PBS and the internalized ^{59}Fe was determined *via* established methods by incubating the cell monolayer for 30 min/4°C with the general protease, Pronase (1 mg/mL; Sigma-Aldrich). The cells were then removed from the monolayer with a plastic spatula and centrifuged for 1 min/12,000×*g*. The supernatant represents membrane-bound, Pronase-sensitive ^{59}Fe that was released by the protease, while the Pronase-insensitive fraction represents internalized ^{59}Fe [34,46,47]. The amount of internalized ^{59}Fe was expressed as a percentage of the ^{59}Fe internalized by untreated control cells (100%).

3.8 Ascorbate oxidation assay for analysis of redox activity of iron complexes. The ability of the iron complexes of the novel ligands to mediate the oxidation of a physiological substrate, ascorbate, was examined using an established protocol [46,48]. In brief, L-ascorbic acid (100 μM) was prepared

Table 2. Molecular weights (MW) and calculated n-octanol/water coefficients (log P_{calc}) of the studied analogs.

Chelator	MW (g/mol)	log P_{calc}
SIH	241	1.5
redSIH	243	1.0
redHAPI	257	1.4
redHPPI	271	1.9
BHAPI	334	2.1
BHPPI	348	2.6
2API	240	0.7
7HII	267	1.4
H16	283	2.2
H17	283	2.2
H18	297	2.5
H28	323	3.1

The MW and log P_{calc} values were calculated using ChemBioOffice Ultra 11.0 software. The log P_{calc} is expressed as an average of the results of Crippen's and Viswanadhan's fragmentations and Broto's method.

doi:10.1371/journal.pone.0112059.t002

immediately prior to the experiment and was incubated either alone or in the presence of Fe^{3+} (10 μM; as $FeCl_3$) in a 50-fold molar excess (500 μM) of citrate and chelators (1-60 μM). Chelators were assayed at iron-binding equivalents (IBE) of 0.1 (excess of iron), 1 (iron-chelator complexes with a fully saturated coordination sphere) and 3 (excess of free chelator). The iron chelators, ethylenediaminetetraacetic acid (EDTA) and DFO, were used as positive and negative controls, respectively, as their redox activity has been well characterized [49]. The decrease in absorbance at 265 nm, which is the absorption maximum of ascorbate, was measured using the plate reader described previously after 10 and 40 min of incubation at RT. The decrease in absorbance between the two time points was calculated and expressed as a percentage of the control in the absence of the chelators (100%).

3.9 Protection against oxidative injury and assessment of cytotoxicity. For these experiments, cells were seeded in 96-well plates (TPP) at a density of 10,000 cells/well (H9c2 rat cardiomyoblast) or 5,000 cells/well (MCF-7). H9c2 cells were seeded in the plates 48 h prior to addition of the studied ligands and 24 h prior to the experiments, the medium was changed to serum- and pyruvate-free DMEM (Sigma-Aldrich). The ability of the ligands to protect against oxidative injury was assessed by a simultaneous 24 h incubation with H_2O_2 (200 μM) in the presence and absence of varying concentrations of the chelators. The inherent cytotoxicity of the ligands was studied using the H9c2 cell line after a 72 h incubation. For proliferation studies, MCF-7 cells were seeded 24 h prior to addition of the chelators. The cytotoxic effects of the various iron chelators were then studied at different concentrations after a 72 h incubation. To dissolve the lipophilic agents, dimethyl sulfoxide (DMSO; Sigma-Aldrich) was utilized leading to a final DMSO concentration of 0.1% (v/v) in the culture medium of all groups. At this concentration, DMSO had no effect on cytotoxicity (data not shown). The viability of the H9c2 and MCF-7 cells was determined using the neutral red (NR; Sigma) uptake assay, which is based on the ability of viable cells to incorporate NR into lysosomes [33,50]. The optical density of soluble NR was measured at $\lambda = 540$ nm using the Tecan Infinite 200 M plate reader. The viability or proliferation of the experimental groups was expressed as a percentage of the untreated controls (100%). Control experiments using viable cell counts demonstrated a direct correlation to NR uptake.

3.10 Data analysis and statistics. The values of the molecular weights (MW) and n-octanol/water coefficients (log P_{calc}; Table 2) were calculated using ChemBioOffice Ultra 11.0 software (CambridgeSoft, Cambridge, MA, USA). The log P_{calc} is expressed as an average of the results of Crippen's [51], Viswanadhan's [52], and Broto's [53] method. SigmaStat for Windows 3.5 (Systat Software, San Jose, CA, USA) statistical software was used for data analyses. The data are expressed as the mean ±S.D. of at least 3 experiments. Statistical significance was determined using a one-way ANOVA with a Bonferroni *post-hoc* test (comparisons of multiple groups against the relevant control). The results were considered to be statistically significant when $p < 0.05$. The EC_{50} (half-maximal effective concentration) and IC_{50} (half-maximal inhibitory concentration) values were calculated using CalcuSyn 2.0 software (Biosoft, Cambridge, UK). Raw data underlying the findings in this study are in Data S1.

Results

1 Stability of the chelators in plasma

The stabilities of the newly prepared chelators in rabbit plasma were studied using HPLC analysis following a 600 min (10 h) incubation *in vitro*. The results were expressed as a percentage of the initial concentration of chelators at time $t = 0$ min. In our previous studies, SIH showed low stability, with less than 10% of SIH remaining intact after 180 min [33] and this was confirmed in our present investigation (Fig. 2A). The methylated and ethylated analogs of SIH, namely HAPI and HPPI, were markedly more resistant than SIH to hydrolysis in plasma. In fact, HAPI and HPPI were present at 26% and 41% of their original concentration at $t = 600$ min [33].

The reduction of the hydrazone bond of SIH caused a marked increase in the stability of redSIH, with 30% of the intact ligand remaining at $t = 600$ min (Fig. 2B). On the other hand, the reduction of the hydrazone bond of HAPI and HPPI, led to comparable or slightly decreased stability relative to SIH, with 23% of redHAPI and 25% of redHPPI remaining intact in plasma at $t = 600$ min (Fig. 2C, D). The bromination of HAPI increased the stability of BHAPI relative to SIH, with 45% of the ligand

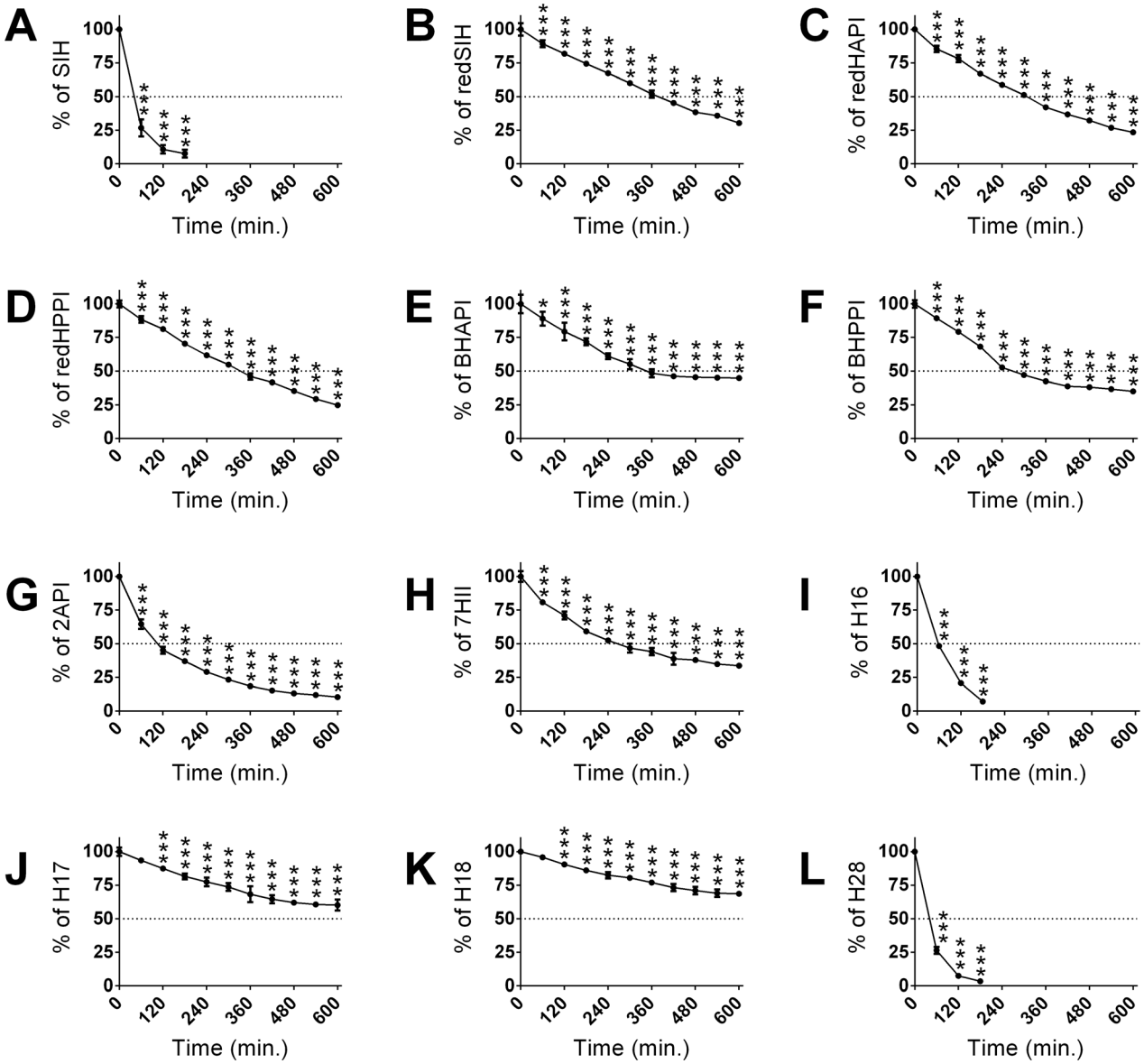

Figure 2. Stabilities of SIH and its novel analogs in rabbit plasma. SIH (**A**), redSIH (**B**), redHAPI (**C**), redHPPI (**D**), BHAPI (**E**), BHPPI (**F**), 2API (**G**), 7HII (**H**), H16 (**I**), H17 (**J**), H18 (**K**) and H28 (**L**) were incubated at 37°C in rabbit plasma and their concentrations were analyzed using HPLC every 60 min until $t = 600$ min. Results are expressed as a percentage of the concentration at $t = 0$ min (100 μM). Results are Mean ±SD ($n = 3$ experiments). Statistical significance (ANOVA): * $p<0.05$, ** $p<0.01$, *** $p<0.001$ compared to the concentration at $t = 0$ min (100%).
doi:10.1371/journal.pone.0112059.g002

remaining intact, while the bromination of HPPI had no significant effect relative to SIH (*i.e.*, 35% of BHPPI remained intact at the end of the 600 min incubation period; Fig. 2E, F).

The 2-acetylpyridine derivative, 2API, showed better stability than the parent chelator, SIH, but was less stable than HAPI, with 10% of 2API remaining intact after the 600 min incubation (Fig. 2G). The cyclic ligand, 7HII, possessed comparable stability to HPPI, with 34% of 7HII remaining at the end of incubation (Fig. 2H). The introduction of a bulky isopropyl or cyclohexyl group to analogs H16 and H28, respectively, resulted in a surprisingly short half-life in plasma, with almost complete decomposition of these ligands at $t = 180$ min (Fig. 2I, L). Pilot experiments showed that the rapid decomposition of H16 was only partially due to hydrolysis of the hydrazone bond (only 10% of the expected ketone was found in plasma), with the instability probably also involving the hydrazine bond. Nevertheless, this remains to be carefully elucidated by using additional advanced analytical methods. In contrast, the introduction of an unbranched propyl or terminally-branched isobutyl moiety (ligands H17 and H18, respectively) led to a pronounced increase of their stability in plasma relative to SIH (Fig. 2 J, K), with 60% of H17 and 69% of H18 remaining intact in plasma after a 10 h incubation.

2. Determination of the iron chelating efficacy in solution and in MCF-7 cells

To assess the iron chelation efficacy of the ligands in solution, the iron complexes of the weak iron chelator, calcein, were used. In this assay, the examined chelators compete with calcein for iron and the fluorescence of the free, dequenched calcein is proportional to their chelation efficacy in comparison to calcein. The iron

chelation efficacy of the novel ligands was expressed as a percentage of the level of calcein de-quenching caused by the parent chelator, SIH (100%).

The reduction of the hydrazone bond in redSIH, redHAPI and redHPPI resulted in significantly ($p<0.001$) reduced iron chelating efficacies in solution (Fig. 3A). The brominated ligands, BHAPI and BHPPI, and the alkylated analogs, 7HII, H17 and H18 exhibited iron chelating activity similar to the reference agent, SIH (Fig. 3A). The 2-acetylpyridine derivative, 2API, was observed to have poor iron chelating efficacy in this assay relative to SIH. However, this may be due to the ability of the iron complex of 2API to oxidize calcein [54], as the iron complex of 2API was identified to act as a pro-oxidant (see below), and thus, resulted in decreased calcein fluorescence. Additionally, low chelation efficacy was also observed for the ligands, H16 and H28 (Fig. 3A), that possess an isopropyl or cyclohexyl group, respectively, adjacent to the hydrazone bond.

The efficacy of the ligands to permeate the cell membrane to gain access to the LIP was examined using the calcein-AM assay in iron-loaded MCF-7 cells (Fig. 3B). In these studies, the iron chelation efficacy of the synthesized ligands was expressed as a percentage of the efficiency of the parent chelator, SIH (100%). The ability of the chelators, BHPPI, 7HII and H17 to permeate the cell membrane and to bind iron from the calcein-AM detectable LIP did not significantly ($p>0.05$) differ from that of SIH (Fig. 3B). This was well correlated with their high chelation efficacy in solution (Fig. 3A). The ligands, redSIH, BHAPI, 2API, H18 and H28, exhibited moderate (50–80% relative to SIH), but significantly ($p<0.05$–0.001) decreased iron chelation efficacy in MCF-7 cells relative to SIH (Fig. 3B). In contrast, redHAPI, redHPPI and H16 displayed the poorest ability (<50% relative to SIH) to access and bind iron from the LIP (Fig. 3B) and this was in good correlation to their chelation activity in solution (Fig. 3A).

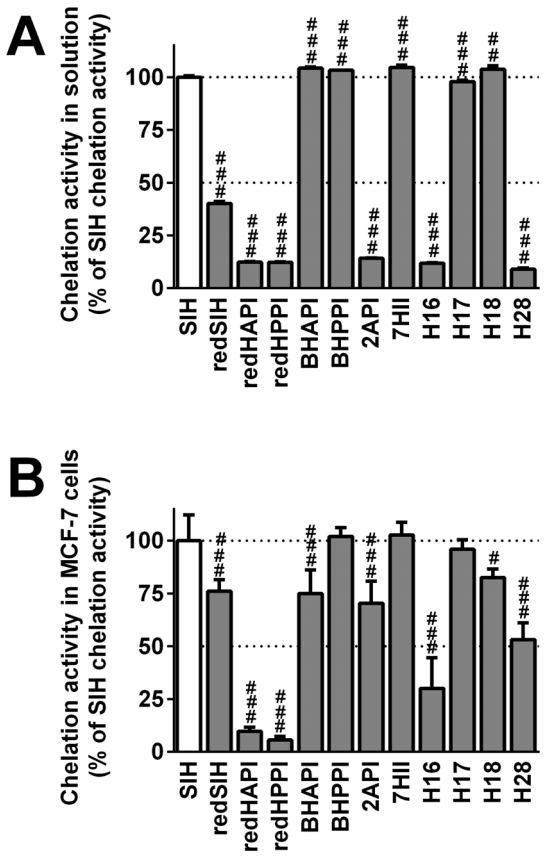

Figure 3. Iron chelation properties of the novel analogs in solution (A) and in MCF-7 cells (B). (**A**) The chelation dynamics of the new agents in solution were observed for 360 s using the calcein assay, and the agent was applied at $t = 100$ s. The fluorescence intensity of free calcein at $t = 360$ s was expressed as a percentage of that observed using the reference iron chelator, SIH. (**B**) The ability of the analogs to chelate "free" iron from the LIP in MCF-7 cells was measured using the calcein-AM assay. The fluorescence intensity of free calcein at $t = 600$ s was expressed as a percentage of that observed in the presence of SIH. Results are Mean ±SD ($n \geq 3$ experiments). Statistical significance (ANOVA): # $p<0.05$, ## $p<0.01$, ### $p<0.001$ compared to the reference chelator, SIH.
doi:10.1371/journal.pone.0112059.g003

3. The effect of the chelators on the mobilization of cellular 59Fe and prevention of cellular 59Fe uptake from 59Fe2-Tf

To examine the ability of the novel ligands to mobilize intracellular ^{59}Fe from MCF-7 cells, ^{59}Fe efflux experiments were performed using established techniques [34,45]. The novel ligands were compared to control medium containing no added chelator and also to the parent analog, SIH (Fig. 4A). The control medium showed limited ability to mobilize cellular ^{59}Fe, resulting in the release of 8% of cellular ^{59}Fe (Fig. 4A). In contrast, SIH displayed high ^{59}Fe mobilization efficacy, mediating the release of 55% of cellular ^{59}Fe (Fig. 4A). The ligands, BHAPI, BHPPI, 2API, 7HII, H17 and H18 were highly effective in mediating ^{59}Fe mobilization and resulted in the release of 43–58% of cellular ^{59}Fe (Fig. 4A). The agents, redSIH and H28 demonstrated significantly ($p<0.001$) increased ^{59}Fe mobilization compared to the control. However, their ^{59}Fe mobilization efficacy was approximately half that of SIH (Fig. 4A). The ^{59}Fe mobilization efficacy of redHAPI, redHPPI and H16 were poor and comparable to the untreated control (Fig. 4A). In general, the results of this assay correlated well with the observed iron-chelation efficacies of these analogs in solution (Fig. 3A) and in the cell-based calcein-AM assay (Fig. 3B). The only notable exception was 2API, which demonstrated high activity at mobilizing cellular ^{59}Fe (Fig. 4A), which was in contrast to the iron chelation assay in solution (Fig. 3A). As noted previously, this could be due to its pro-oxidative effects on calcein [54].

As the iron chelation efficacy and cytotoxic activity of a ligand are due to both its ability to mobilize cellular Fe, but also, inhibit Fe uptake from Tf [34], the ability of the chelators to prevent the cellular uptake of ^{59}Fe from $^{59}Fe_2$-Tf was determined and expressed as a percentage of the untreated control (Fig. 4B). As observed in the ^{59}Fe mobilization experiments, the parent chelator, SIH, demonstrated high ^{59}Fe chelation efficacy and inhibited ^{59}Fe uptake to 15% of the control (Fig. 4B).

Importantly, those ligands that showed high ^{59}Fe mobilization efficacy (Fig. 4A) were also highly effective at inhibiting the uptake of ^{59}Fe from $^{59}Fe_2$-Tf (Fig. 4B). For example, the ligands, BHAPI, BHPPI, 2API, 7HII, H17 and H18, that demonstrated high ^{59}Fe mobilization activity, were able to limit ^{59}Fe uptake to 10–26% of the control (Fig. 4B). In contrast, the compounds, redSIH, redHAPI, redHPPI, H16, and H28, showed limited ability to prevent ^{59}Fe uptake, inhibiting it to>70% of the control (Fig. 4B).

4. Examination of the ability of the iron-chelator complexes to catalyze the oxidation of ascorbate

It has been previously observed that the cytotoxic effects of some iron chelators is due not only to their ability to bind cellular iron, but also to form redox-active iron complexes [12,46,55]. Thus, we examined whether the iron complexes of our novel

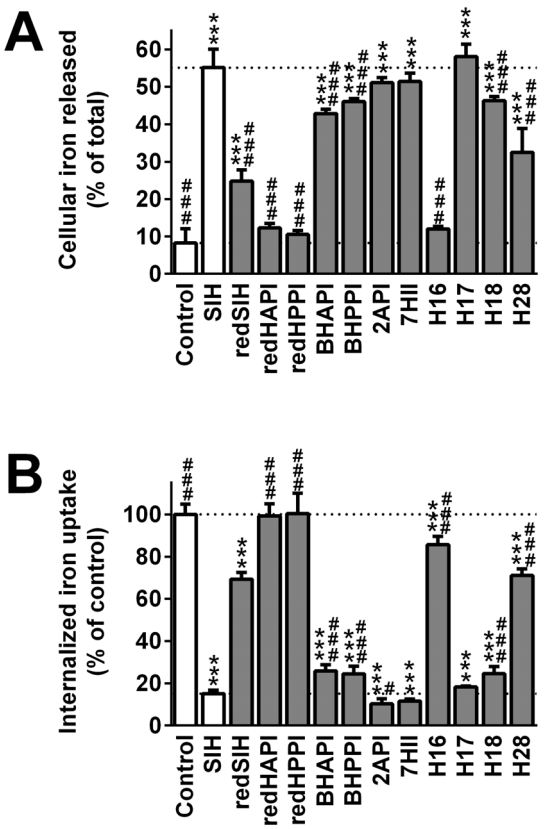

Figure 4. The effect of SIH and its analogs on ^{59}Fe mobilization from pre-labeled MCF-7 cells (A) and on internalized ^{59}Fe uptake from $^{59}Fe_2$-transferrin (Tf) by MCF-7 cells (B). (**A**) The ability of the ligands to promote ^{59}Fe mobilization from MCF-7 cells was performed by first prelabeling the cells with $^{59}Fe_2$-Tf (0.75 μM) for 3 h/37°C, followed by washing and then reincubation for 3 h/37°C with either control medium alone, or control medium containing the chelator (25 μM). (**B**) Inhibition of ^{59}Fe uptake from $^{59}Fe_2$-Tf by MCF-7 cells by chelators was performed by incubating cells for 3 h/37°C with $^{59}Fe_2$-Tf (0.75 μM) in the presence or absence of the chelator (25 μM). Results are Mean ±SD ($n \geq 3$ experiments). Statistical significance (ANOVA): * $p<0.05$, ** $p<0.01$, *** $p<0.001$ compared to the control (untreated) group, and # $p<0.05$, ## $p<0.01$, ### $p<0.001$ compared to the reference chelator, SIH.
doi:10.1371/journal.pone.0112059.g004

ligands were able to redox cycle by assessing their ability to mediate the oxidation of ascorbate by standard methods [46,48]. The ability of the iron complexes to catalyze the oxidation of ascorbate was expressed as a percentage of the control (ascorbate with "free" Fe^{3+}).

The chelators, DFO and EDTA, were used as negative (anti-oxidative) and positive (pro-oxidative) controls, respectively [46,49]. As previously observed, the Fe complex of DFO demonstrated a typical anti-oxidative profile [56], resulting in decreased levels of ascorbate oxidation at an IBE of 3 (excess DFO) than at an IBE of 0.1 (excess iron; Fig. 5). In contrast, the iron complex of EDTA exhibited a pro-oxidative effect and mediated higher levels of ascorbate oxidation at an IBE of 3 relative to that at 0.1 (Fig. 5). In fact, at an IBE of 3, the iron complex of EDTA increased the oxidation of ascorbate to 924% of the control.

The iron complex of the parent chelator, SIH, exhibited anti-oxidant activity similar to that of the iron complex of DFO (Fig. 5). All of the iron complexes of the novel ligands, with the exception of 2API, demonstrated neither anti-oxidant nor pro-oxidative effects and were comparable to the control. The iron complex of the pyridine derivative, 2API, was the only Fe complex that showed pro-oxidative effects and significantly ($p<0.001$) increased ascorbate oxidation to 256% relative to the control at an IBE of 3 (Fig. 5).

5. Prevention of oxidative injury induced by hydrogen peroxide

The ability of the ligands to act as protective agents in a model of oxidative stress was then examined by assessing the cellular viability of H9c2 cardiomyoblast cells upon a 24 h co-incubation of the chelators with H_2O_2 (200 μM). These results are shown in Fig. 6 and summarized in Table 3. In these experiments, the EC_{50} value is calculated which represents the concentration that reduced the cytotoxicity induced by hydrogen peroxide (200 μM) to 50% of the untreated control after a 24 h/37°C incubation with H9c2 cells. SIH was used as a positive control and resulted in an EC_{50} value of 7.63±1.38 μM (Table 3).

Of all the novel ligands synthesized, the analog that displayed the highest level of cytoprotective activity was 7HII, with an EC_{50} value of 2.68±1.30 μM (Table 3). In fact, 7HII demonstrated significantly ($p<0.001$) greater protection against hydrogen peroxide-induced cytotoxicity than the parent chelator, SIH. Although the iron chelators, BHAPI, BHPPI, 2API, H17 and H18 also prevented peroxide-induced cytotoxicity (EC_{50}: 8.48–42.57 μM), their EC_{50} values were higher than that of SIH. The ligands, redSIH, redHAPI, redHPPI, H16 and H28 did not display protective activity against peroxide-induced cytotoxicity in the concentration range examined.

6. Cytotoxicity studies in H9c2 cardiomyoblast cells

The selectivity of the novel ligands was then examined after a 72 h incubation with the non-tumorigenic H9c2 cardiomyoblast cell line (Fig. 7; Table 3). The parent chelator, SIH, was examined as a control and demonstrated an IC_{50} value of 49.47±1.77 μM (Table 3).

Of the synthesized analogs, redHAPI, redHPPI, H16 and H28 were the least toxic agents, with IC_{50} values>80 μM. The ligands, redSIH and H17, showed comparable cytotoxicity to H9c2 cardiomyoblasts as the parent chelator, SIH. The other studied ligands, BHAPI, BHPPI, 2API, 7HII, H18, were more toxic than the chelator, SIH, with IC_{50} values ranging from 0.62 μM to 7.40 μM. The most cytotoxic agent was 7HII with an IC_{50} value of 0.62±0.17 μM (Table 3; Fig. 7).

7. Cytotoxic effects of SIH derivatives on MCF-7 cells

The cytotoxic effects of the SIH derivatives were studied in MCF-7 breast adenocarcinoma cells following a 72 h incubation. The parent chelator, SIH, was used as a control and demonstrated moderate cytotoxic activity (IC_{50}: 4.21±1.05 μM; Table 3; Fig. 8), similar to that previously observed [31].

The analogs containing a reduced hydrazone bond (redSIH, redHAPI and redHPPI) or an isopropyl group adjacent to this bond (H16) exhibited poor cytotoxic activity (IC_{50}>100 μM). The chelator, H28, with a bulky cyclohexyl group in close proximity to the hydrazone bond demonstrated intermediate cytotoxic effects, with an IC_{50} of 42.41±3.15 μM. The remaining agents, BHAPI, BHPPI, 2API, 7HII, H17 and H18, showed increased cytotoxic activity (IC_{50}: 0.38–2.92 μM; Table 3) relative to SIH (Table 3). The greatest level of cytotoxic activity was observed with the indanone derivative, 7HII (IC_{50} = 0.38±0.11 μM).

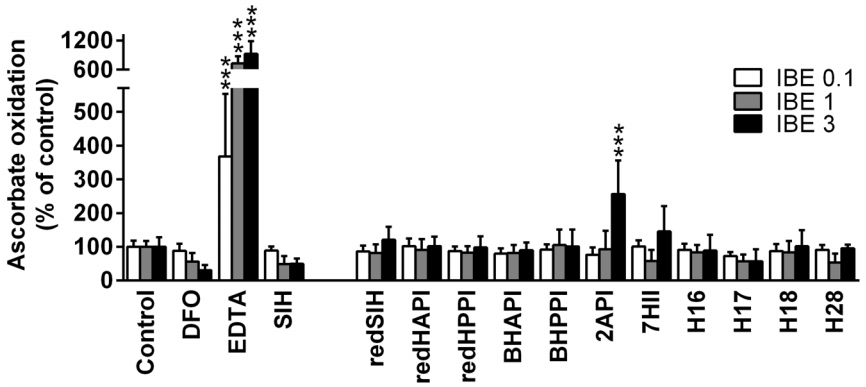

Figure 5. Effects of SIH and its analogs on iron-induced oxidation of ascorbic acid in a buffered solution (pH 7.4). Chelators were assayed at iron binding equivalents (IBE) of 0.1 (excess of Fe), 1 (iron-chelator complexes with a fully filled coordination sphere) and 3 (excess of free chelator). DFO and EDTA were used as negative and positive control chelators, respectively. The results are expressed as a percentage of the control group in the absence of chelator (100%). Results are Mean ±SD ($n \geq 3$ experiments). Statistical significance (ANOVA): * $p<0.05$, ** $p<0.01$, *** $p<0.001$ as compared to the control group (iron with ascorbate).
doi:10.1371/journal.pone.0112059.g005

To provide insight into the selectivity of the cytotoxic effects of the novel ligands, which is crucial for potential anti-cancer agents, their IC_{50} values in H9c2 cells and their IC_{50} values in MCF-7 cells were compared by calculating a "selectivity ratio", namely IC_{50} H9c2/IC_{50} MCF-7 cells (Table 3). SIH had a selectivity ratio of 11.75. The analogs, redSIH and redHAPI, with reduced hydrazone bonds had lower IC_{50} values in H9c2 cardiomyoblasts than in MCF-7 cancer cells, indicating greater cytotoxic activity in the former. Relative to SIH, this resulted in a marked decrease in the selectivity ratio to 0.14 and 0.63, respectively (Table 3). The ligands, redHPPI, 2API, 7HII and H28, showed somewhat similar cytotoxic activity in both the MCF-7 and H9c2 cell-types leading to selectivity ratios that were far less than SIH, and which ranged between 1.05 and 2.01. On the other hand, the bromine-substituted chelators (BHAPI and BHPPI) demonstrated selective activity against MCF-7 breast cancer cells relative to the H9c2 cell-type, although their selectivity ratios were approximately half that observed for SIH, *viz.*, 6.59 and 7.60, respectively (Table 3). The analogs that demonstrated the greatest selectivity profile against MCF-7 cells relative to H9c2 cells were the propyl (H17) and isobutyl (H18) derivatives of SIH, which were more active than SIH itself, demonstrating selectivity ratios of 14.36 and 15.10, respectively (Table 3).

Discussion

Aroylhydrazones represent an intriguing group of chelators that exhibit a variety of biological effects associated with their ability to influence cellular iron levels [27,33,57]. The aim of the present study was to synthesize and evaluate the biological activity of a series of new analogs of the well-established iron-binding ligand, SIH, with respect to their: (***1***) stability in plasma, (***2***) cytotoxic effects; (***3***) ability to protect cells against oxidative injury; and (***4***) cytotoxicity to H9c2 non-tumorigenic cardiomyoblast cells. The iron chelation activity, ability to mobilize cellular ^{59}Fe, efficacy to inhibit ^{59}Fe uptake from $^{59}Fe_2$-Tf, and the redox activity of the iron complexes of the novel analogs were also determined, as these properties are crucial factors involved in their biological activity [34,35]. The primary goal was to further characterize the structure-activity relationships of SIH-related aroylhydrazones for the future rational design of compounds with therapeutic potential.

1. Reduction of the hydrazone bond

First, we probed the role of the hydrazone bond itself, as it is prone to hydrolysis and is a site of instability in this class of compounds [58]. Previous studies suggested that structurally-related compounds with a reduced C = N bond retained their chelation properties [59]. In fact, these reduced compounds inhibited the iron-induced generation of hydroxyl radicals and protected murine dermal fibroblasts against UV-induced lipid peroxidation and UV-induced cytotoxicity [59]. Thus, we examined the effect of the reduction of the hydrazone bond of the chelators, SIH, HAPI and HPPI, as these ligands previously exhibited cardioprotective [33] and cytotoxic [31] activity.

The results of the present study revealed that the reduced analogs were relatively non-toxic against both tumorigenic MCF-7 cells and non-tumorigenic H9c2 cardiomyoblasts (Table 3). The cytotoxicity of redHAPI and redHPPI were approximately one order of magnitude lower than those of the parent chelators (HAPI and HPPI, respectively) [31,33], while the cytotoxic activity of redSIH towards H9c2 cells was similar to that of SIH (Table 3). This effect could be caused by the increased stability of redSIH (Fig. 2B) compared to SIH (Fig 2A), and therefore, the prolonged exposure of cells to intact redSIH compensated for the reduced (yet significant) iron chelation activity. Reduction of the hydrogen bond in redSIH, redHAPI and redHPPI led to a marked decrease in their selectivity ratios (0.14–1.14) relative to SIH (11.75; Table 3). In fact, these agents containing a reduced hydrazone bond had the lowest selectivity ratios of all analogues examined in this investigation. Furthermore, these latter compounds lost the ability to protect H9c2 cells against oxidative stress relative to SIH (Table 3) [33]. This lack of protection against oxidative stress is likely due to their limited iron chelation (Fig. 3) and ^{59}Fe mobilization efficacy (Fig. 4A). Of the reduced analogs, only redSIH retained limited chelation activity (Figs. 3 and 4). Therefore, the presence of the hydrazone bond is an important criterion for the cardioprotective and cytotoxic effects of these aroylhydrazones. The loss of iron chelation efficacy of the reduced analogs may be a result of the altered molecular spatial arrangement of the ligating groups due to the free rotation of the single C-N bond, or the decreased electron density on the chelating nitrogen due to its transition from sp^2 to sp^3 orbital hybridization.

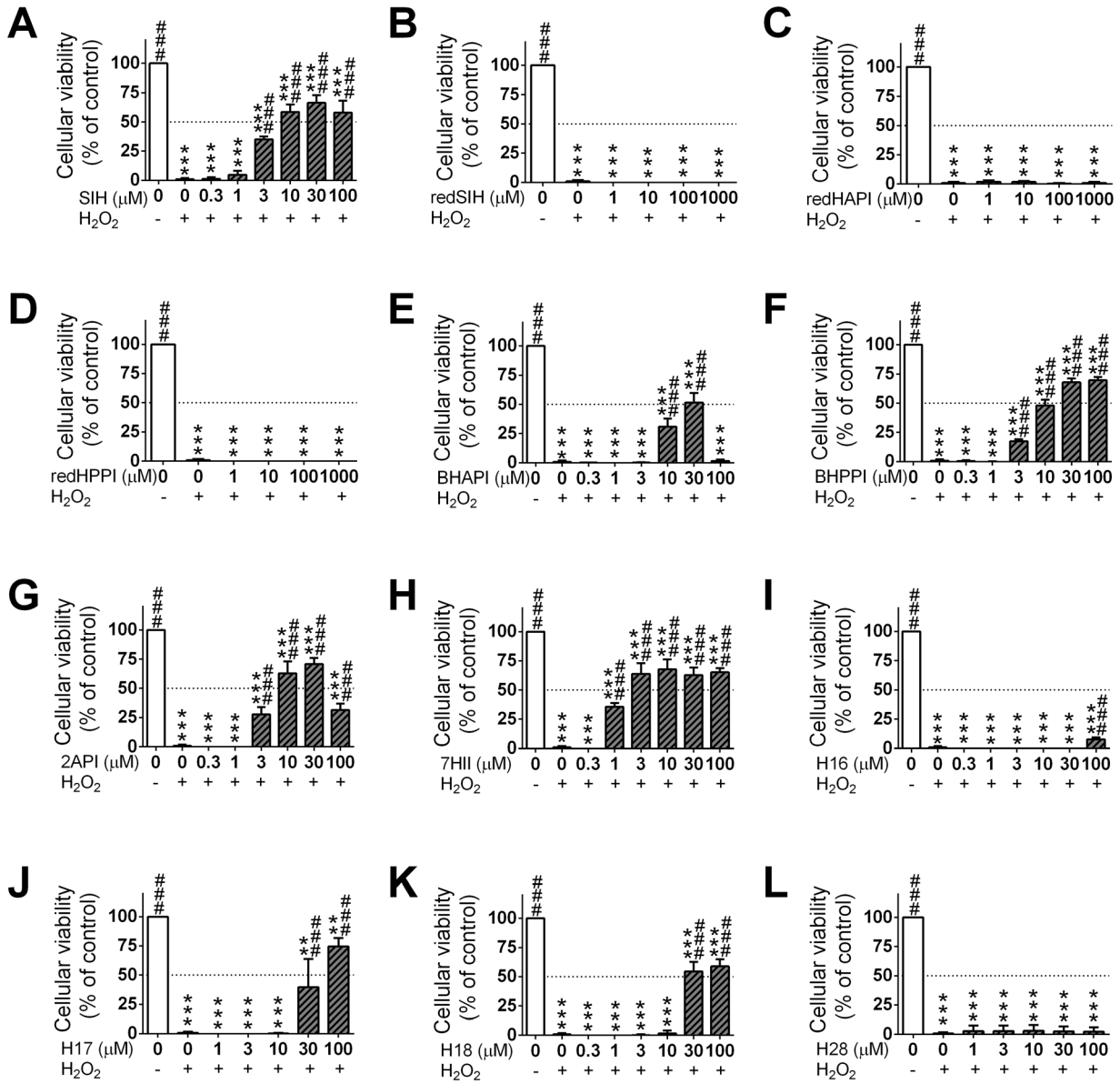

Figure 6. Protective effects of the chelator, SIH (A), and the new analogues (B–L). The ability of the SIH derivatives to protect H9c2 cardiomyoblast cells against oxidative injury were evaluated using a 24 h/37°C incubation of the cells with H_2O_2 (200 μM) and the novel analogs (0.3–1000 μM). Results are Mean ±SD ($n \geq 4$ experiments). Statistical significance (ANOVA): * $p<0.05$, ** $p<0.01$, *** $p<0.001$ compared to the control (untreated) group, and # $p<0.05$, ## $p<0.01$, ### $p<0.001$ compared to the H_2O_2 group.
doi:10.1371/journal.pone.0112059.g006

2. Bromination of the phenyl ring

The introduction of a halogen into the structure of a molecule enhances its lipophilicity (Table 2), which can potentially facilitate its permeation into cells. The halogen substitution, due to its inductive electron-withdrawing effects, may also influence the stability of the hydrazone bond and the ability of the compound to chelate metal ions. Indeed, a previously synthesized chlorinated HAPI derivative (*i.e.*, (*E*)-*N′*-[1-(5-chloro-2-hydroxyphenyl)ethylidene]isonicotinoylhydrazide; CHAPI), showed greater hydrolytic stability than HAPI and moderate cytotoxic activity ($IC_{50} = 0.65 \pm 0.07$ μM against MCF-7 cells) [31]. Therefore, the brominated analog, BHAPI, bearing a bromine instead of chlorine, and its homolog, BHPPI (Fig. 1), was prepared to evaluate the influence of halogenation on the cardioprotective and cytotoxic activity of these chelators. The stability of BHAPI and BHPPI was similar to the chloro derivative, CHAPI. However, the presence of bromine instead of the chlorine substituent increased the chelating efficiency of these compounds in cells from approximately 50% for CHAPI, to 75% and 100% for BHAPI and BHPPI, respectively. Both BHAPI and BHPPI showed comparable iron chelation efficacy to SIH in solution, as well as in cells (Fig. 3). The cytotoxic activity of these brominated analogs against MCF-7 cells was greater than that found for SIH (Table 3). Further, both BHAPI and BHPPI showed greater cytotoxic activity against MCF-7 breast cancer cells relative to non-tumorigenic, H9c2 cardiomyoblasts, although their selectivity ratios were approximately half that observed for SIH (Table 3). In addition, BHAPI and BHPPI were less effective than SIH when assessing the ability of these agents to prevent the cytotoxicity

Table 3. Protective and cytotoxic effects of the synthesized SIH derivatives and their calculated "selectivity ratios".

Chelator	EC_{50} H9c2 (μM)	IC_{50} H9c2 (μM)	IC_{50} MCF-7 (μM)	Selectivity Ratio
SIH	7.63±1.38	49.47±1.77	4.21±1.05	11.75
redSIH	N/A	39.59±5.11	279.97±53.17	0.14
redHAPI	N/A	83.96±2.76	133.47±28.76	0.63
redHPPI	N/A	226.12±6.31	197.86±13.09	1.14
BHAPI	30.34±7.23	6.99±0.82	1.06±0.46	6.59
BHPPI	17.18±4.39	6.31±0.59	0.83±0.50	7.60
2API	8.48±3.11	3.07±0.55	2.92±0.67	1.05
7HII	2.68±1.30	0.62±0.17	0.38±0.11	1.63
H16	N/A	>100	153.67±24.20	-
H17	42.57±7.94	32.60±1.09	2.27±0.14	14.36
H18	27.76±3.90	7.40±2.13	0.49±0.18	15.10
H28	N/A	85.37±12.90	42.41±3.15	2.01

The EC_{50} values (concentration that reduced the cytotoxicity induced by H_2O_2 (200 μM) to 50% of the untreated control) were calculated after a 24 h incubation with non-tumorigenic H9c2 cardiomyoblasts. The IC_{50} values (concentration that reduced the cellular viability or proliferation to 50% of the untreated control) were calculated after a 72 h incubation with H9c2 cardiomyoblasts or MCF-7 breast cancer cells. Selectivity ratios were calculated *via* IC_{50} H9c2 cells/IC_{50} MCF-7 cells. Mean ± SD; $n \geq 4$ experiments. N/A - the EC_{50} value was not achieved within the studied concentration range (no protection).

doi:10.1371/journal.pone.0112059.t003

induced by H_2O_2 in H9c2 cardiomyoblasts (Table 3). Similar results were previously observed for the chlorine derivative, CHAPI [33].

3. Exchange of phenol for pyridine

The ligand, 2API, which contains a pyridine nitrogen as a donor atom instead of the phenolic oxygen, was prepared to examine the effect of alterations of the donor atom set from *O*, *N*, *O* to *N*, *N*, *O* on their biological activity. The main reason for this structural modification was that exchanging a hard base ligand (phenolic oxygen) for a softer base (nitrogen) could markedly alter the ability of such a compound to bind Fe^{3+}/Fe^{2+}. In addition, structurally similar hydrazones derived from pyridine-2-carbaldehyde gained attention in the treatment of iron overload diseases [37,38]. The cytotoxic activity of 2API was similar in MCF-7 breast cancer cells and non-tumorigenic H9c2 cells, with the selectivity ratio decreasing markedly (to 1.05) relative to that observed with SIH (11.75; Table 3). This observation may be explained by the redox activity of 2API, as it was the only analog that exhibited significant pro-oxidative activity in the ascorbate oxidation assay (Fig. 5). In fact, previous studies reported the reversible $Fe^{2+/3+}$ redox couple of the iron complex of 2API [60] and the current investigation demonstrates its ability to oxidize ascorbate.

The iron chelation efficacy and ^{59}Fe mobilization activity of 2API in cells was marked, with the ligand being generally comparable to SIH (Figs. 3B, 4A, 4B). In contrast, the iron chelation activity of 2API in solution did not correlate with the results of cellular experiments (Fig. 3A), which may be explained by the pro-oxidative effects of 2API. It is possible the ability of the 2API iron complex to redox cycle may have interfered in the solution-based calcein assay, as it is known that the fluorescence of free calcein decreases in an oxidative environment [54]. Whereas the unaltered sensitivity of the calcein-AM assay in cells (Fig. 3B) with regards to 2API, may be due to the redox buffering capacity provided by glutathione and other intracellular anti-oxidative systems [61] that maintain calcein sensitivity. In summary, the alteration of the donor atom set from *O*, *N*, *O* to *N*, *N*, *O* in 2API resulted in the formation of a redox active iron complex with decreased selectivity against MCF-7 breast cancer cells. However, the exact mechanism of action of this compound remains to be elucidated.

4. Branching, prolongation or cyclization of the alkyl chain adjacent to the hydrazone bond

In a previous investigation, we found that the presence of an alkyl chain adjacent to the hydrazone bond did not significantly increase the cytotoxic activity of the ketone-derived hydrazones, HAPI and HPPI, compared to SIH [31]. In the current study, we synthesized the analogs, 7HII, H16, H17, H18 and H28, to evaluate the influence of alkyl chain length and branching on biological activity.

The 7-hydroxyindanone derivative, 7HII, contains an extra five-membered ring relative to SIH and showed comparable iron chelating and ^{59}Fe mobilization efficacy (Figs. 3, 4). The cyclization of the alkyl chain, and hence, its increased rigidity, improved its hydrolytic stability (Fig 2H) and also its ability to protect cells against oxidative stress compared to SIH, with 7HII being the most effective ligand screened in this regard (Table 3). However, this structural change in 7HII resulted in significantly higher cytotoxicity towards H9c2 cells and a marked drop in the selectivity ratio relative to SIH (Table 3). Therefore, this structural modification resulted in unfavorable biological activity.

The ligand, H16, bears an additional isopropyl chain at the α-position from the hydrazone bond relative to SIH (Fig. 1). This modification was intended to: (***1***) protect the hydrazone bond against hydrolysis [62]; and (***2***) increase lipophilicity, which is known to enhance cellular permeability of aroylhydrazone ligands [34]. However, this structural modification in H16 resulted in similar stability in plasma as SIH and a marked loss of its iron chelation activity relative to SIH. This effect may be due to steric hindrance around the hydrazone bond mediated by the bulky branched isopropyl group that potentially reduces binding to iron. Notably, consistent with the loss of iron-binding, the cytotoxic activity of H16 was very low in H9c2 and MCF-7 cells and did not show any protective effects against H_2O_2 (Table 3).

To examine whether the effect of the isopropyl chain of H16 was caused by steric hindrance close to the hydrazone bond,

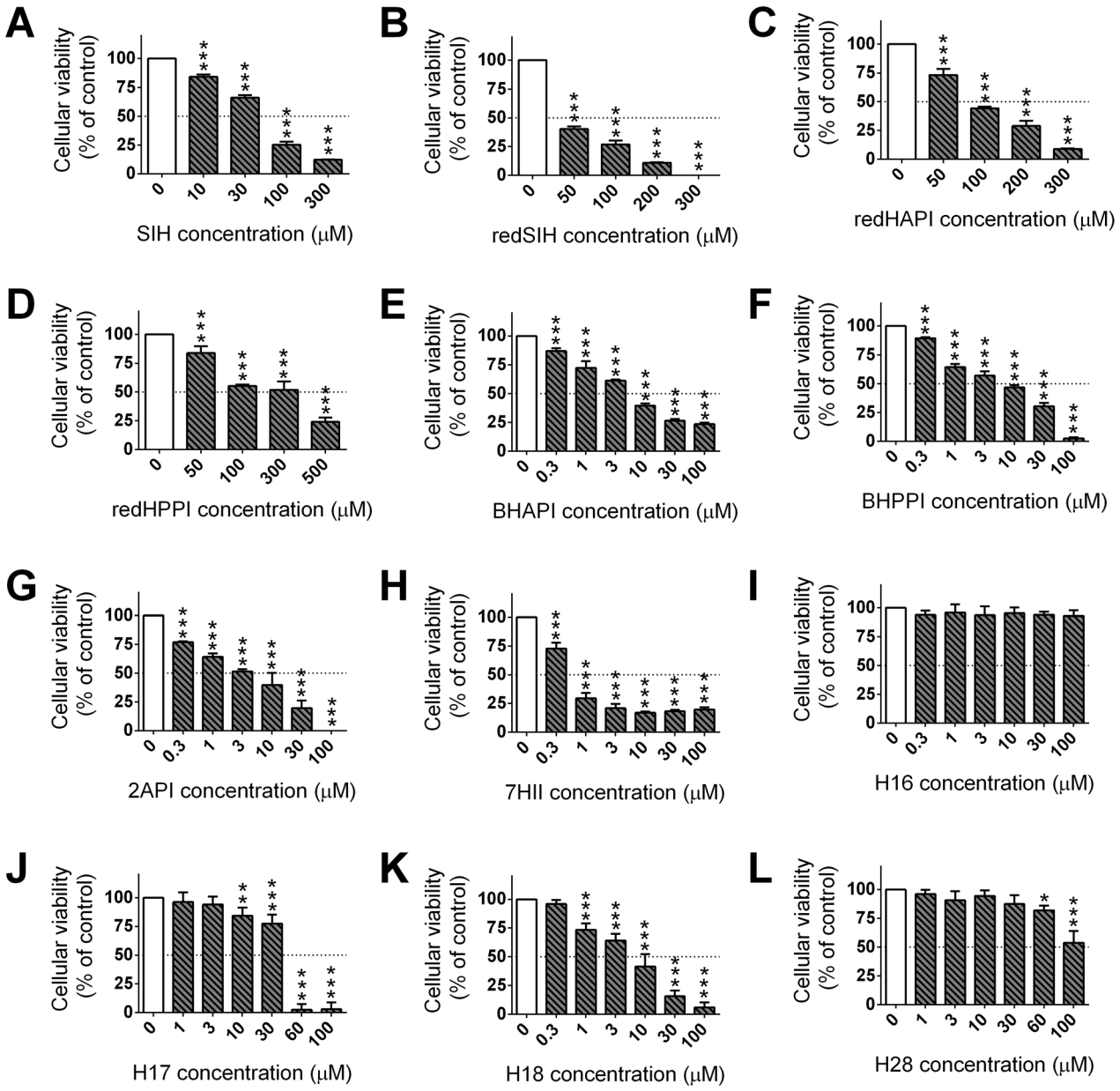

Figure 7. Cytotoxic effects of the chelator, SIH (A), and the new analogues (B–L), using non-tumorigenic H9c2 cardiomyoblasts. The effect of the analogs (0.3–300 μM) on the cellular viability of H9c2 cardiomyoblasts were performed using a 72 h/37°C incubation. Results are Mean ±SD ($n \geq 4$ experiments). Statistical significance (ANOVA): * $p<0.05$, ** $p<0.01$, *** $p<0.001$ as compared to the control (untreated) group.
doi:10.1371/journal.pone.0112059.g007

compound H17, with an unbranched propyl chain, was prepared. Interestingly, this ligand was even more stable in plasma (Fig. 2J) than its homolog HPPI [33]. Furthermore, the iron chelation and ^{59}Fe mobilization efficacy of H17 was similar to SIH, with the compound showing selective cytotoxic activity against MCF-7 cancer cells relative to non-tumorigenic H9c2 cardiomyoblasts [31,33]. In fact, the selectivity ratio of H17 (14.36) was greater than that found for SIH (11.75), demonstrating its potential. We were also interested to examine whether H18, with an isobutyl substituent adjacent to the hydrazone bond (Fig. 1), would retain the favorable activity of H17. In contrast to H16, H18 is branched at the β-position in relation to the imine carbon and led to the ligand maintaining hydrolytic stability, iron chelation efficacy in solution and also in cells relative to SIH (Figs. 2J, 3, 4). This structural change increased the cytotoxic activity of H18 against both MCF-7 tumor cells and H9c2 cardiomyoblasts relative to SIH and H17 (Table 3). However, notably, H18 had the best selectivity ratio of all the studied compounds (*i.e.*, 15.10).

To further examine the structure-activity relationships of bulky substituents close to the hydrazone bond, compound H28, with a cyclohexyl group, was prepared. As in the case of H16, this modification did not improve the low hydrolytic stability observed with SIH (Fig. 2L). Also, the iron chelation efficacy of H28 was markedly decreased (Figs. 3, 4). Furthermore, in comparison with H16, the cytotoxic activity of H28 was greater in both MCF-7 and H9c2 cells, leading to an unfavorable selectivity ratio of 2.01 which was much less than SIH. In addition, the cardioprotective activity

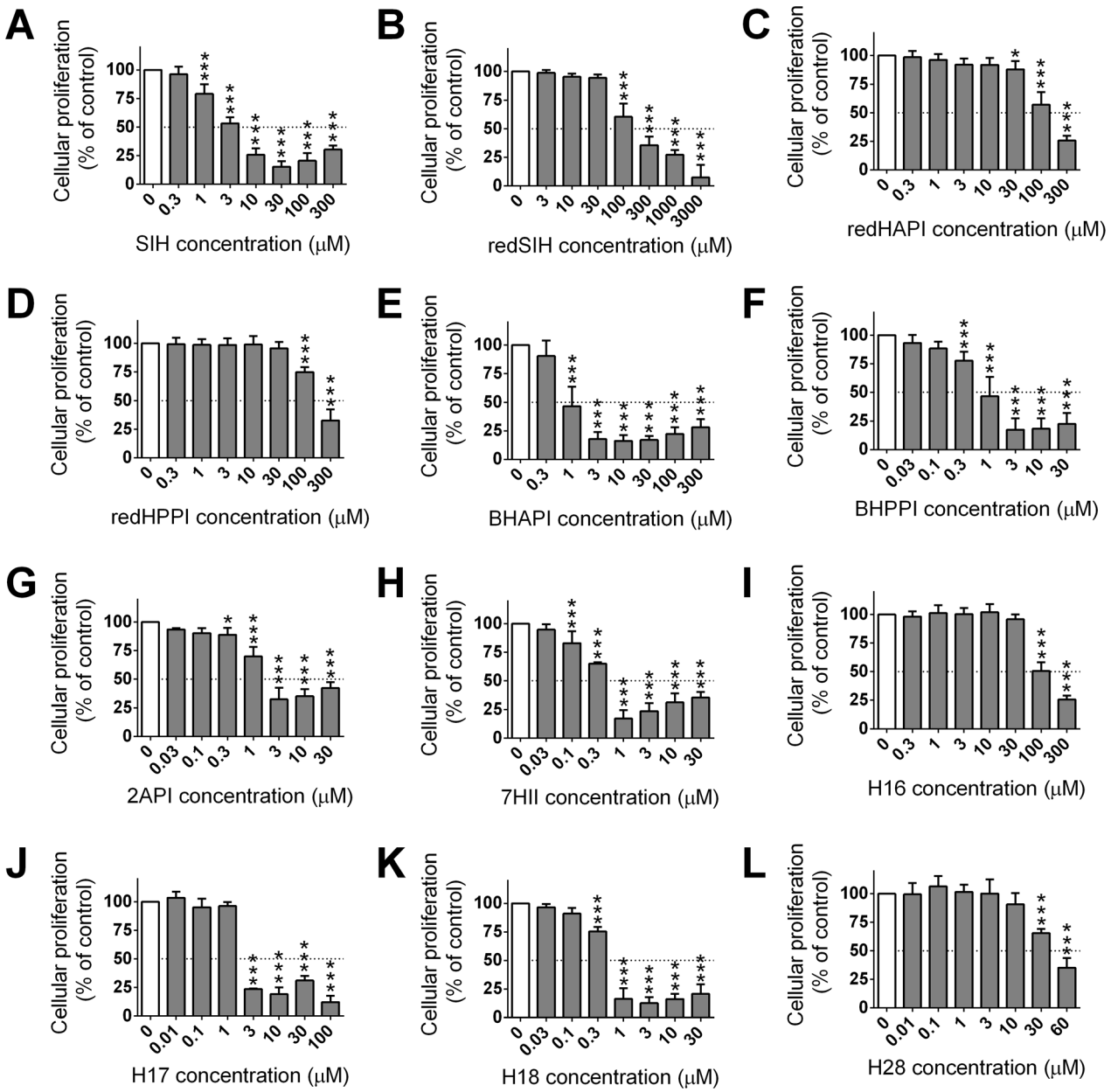

Figure 8. Cytotoxic effects of the chelator, SIH (A), and the new analogues (B–L) against MCF-7 breast cancer cells. For the determination of their cytotoxic activity, MCF-7 breast adenocarcinoma cells were incubated with the analogs (0.01–3000 μM) for 72 h/37°C. Results are Mean ±SD ($n \geq 4$ experiments). Statistical significance (ANOVA): * $p<0.05$, ** $p<0.01$, *** $p<0.001$ as compared to the control (untreated) group.
doi:10.1371/journal.pone.0112059.g008

of H28 against H_2O_2 was completely abolished, which is consistent with the low iron chelation efficacy of H28.

Thus, the alkyl chain on the imine carbon markedly influenced the activity of such hydrazones. Prolonged linear or iso-branched alkyl groups increased their anti-cancer potential, while branching or cyclization in close proximity to the hydrazone bond dramatically decreased their chelation ability and, consequently, decreased their cytotoxic activity against MCF-7 cells and their ability to protect H9c2 cells against oxidative injury.

5. Conclusions

In this study, we identified several structural parameters important for the design of aroylhydrazone iron chelators. First, the hydrazone bond is essential for chelation activity. Second, bromination of the phenyl ring does not have any beneficial effect due to increased non-selective cytotoxic activity against non-tumorigenic H9c2 cardiomyoblasts. Third, exchange of the chelating phenolic hydroxyl (a hard base) for a pyridine nitrogen (softer base) resulted in increased non-selective cytotoxic activity, the mechanism of which is not exactly known. Finally, and most significantly, the exchange of the aldimine hydrogen in SIH for a longer unbranched or iso-branched alkyl group is a favorable modification to increase the stability and anti-cancer potential of such hydrazones. The most promising compounds identified in this study are the propyl-containing analog, H17, and isobutyl-

containing derivative, H18, which possessed the highest selectivity ratios. These compounds warrant further investigation.

Supporting Information

Data S1 Raw data underlying the findings in this study.
(ZIP)

Author Contributions

Conceived and designed the experiments: EP KH JB PK PH DJRL DSK DRR KV TŠ. Performed the experiments: EP KH JB PK IAŠ KP LK TH PH HJ MM AJ VR DJRL. Analyzed the data: EP KH JB PK KV TŠ. Wrote the paper: EP KH JB PK PH DJRL DSK DRR KV TŠ.

References

1. Wang J, Pantopoulos K (2011) Regulation of cellular iron metabolism. Biochem J 434: 365–381.
2. Lawen A, Lane DJ (2013) Mammalian iron homeostasis in health and disease: uptake, storage, transport, and molecular mechanisms of action. Antioxid Redox Signal 18: 2473–2507.
3. Dunn LL, Suryo Rahmanto Y, Richardson DR (2007) Iron uptake and metabolism in the new millennium. Trends Cell Biol 17: 93–100.
4. Hentze MW, Muckenthaler MU, Andrews NC (2004) Balancing acts: molecular control of mammalian iron metabolism. Cell 117: 285–297.
5. Richardson DR, Baker E (1991) The release of iron and transferrin from the human melanoma cell. Biochim Biophys Acta 1091: 294–302.
6. Napier I, Ponka P, Richardson DR (2005) Iron trafficking in the mitochondrion: novel pathways revealed by disease. Blood 105: 1867–1874.
7. Richardson DR, Lane DJ, Becker EM, Huang ML, Whitnall M, et al. (2010) Mitochondrial iron trafficking and the integration of iron metabolism between the mitochondrion and cytosol. Proc Natl Acad Sci U S A 107: 10775–10782.
8. Arredondo M, Nunez MT (2005) Iron and copper metabolism. Mol Aspects Med 26: 313–327.
9. Leidgens S, Bullough KZ, Shi H, Li F, Shakoury-Elizeh M, et al. (2013) Each member of the poly-r(C)-binding protein 1 (PCBP) family exhibits iron chaperone activity toward ferritin. J Biol Chem 288: 17791–17802.
10. Cooper CE, Lynagh GR, Hoyes KP, Hider RC, Cammack R, et al. (1996) The relationship of intracellular iron chelation to the inhibition and regeneration of human ribonucleotide reductase. J Biol Chem 271: 20291–20299.
11. Lane DJ, Mills TM, Shafie NH, Merlot AM, Saleh Moussa R, et al. (2014) Expanding horizons in iron chelation and the treatment of cancer: Role of iron in the regulation of ER stress and the epithelial-mesenchymal transition. Biochim Biophys Acta 1845: 166–181.
12. Kalinowski DS, Richardson DR (2005) The evolution of iron chelators for the treatment of iron overload disease and cancer. Pharmacol Rev 57: 547–583.
13. Merlot AM, Kalinowski DS, Richardson DR (2013) Novel chelators for cancer treatment: where are we now? Antioxid Redox Signal 18: 973–1006.
14. Richardson DR, Kalinowski DS, Lau S, Jansson PJ, Lovejoy DB (2009) Cancer cell iron metabolism and the development of potent iron chelators as anti-tumour agents. Biochim Biophys Acta 1790: 702–717.
15. Bendova P, Mackova E, Haskova P, Vavrova A, Jirkovsky E, et al. (2010) Comparison of clinically used and experimental iron chelators for protection against oxidative stress-induced cellular injury. Chem Res Toxicol 23: 1105–1114.
16. Torti SV, Torti FM (2013) Iron and cancer: more ore to be mined. Nat Rev Cancer 13: 342–355.
17. Kolberg M, Strand KR, Graff P, Andersson KK (2004) Structure, function, and mechanism of ribonucleotide reductases. Biochim Biophys Acta 1699: 1–34.
18. Walker RA, Day SJ (1986) Transferrin receptor expression in non-malignant and malignant human breast tissue. J Pathol 148: 217–224.
19. Jiang XP, Elliott RL, Head JF (2010) Manipulation of iron transporter genes results in the suppression of human and mouse mammary adenocarcinomas. Anticancer Res 30: 759–765.
20. Pinnix ZK, Miller LD, Wang W, D'Agostino R, Jr., Kute T, et al. (2010) Ferroportin and iron regulation in breast cancer progression and prognosis. Sci Transl Med 2: 43ra56.
21. Le NT, Richardson DR (2002) The role of iron in cell cycle progression and the proliferation of neoplastic cells. Biochim Biophys Acta 1603: 31–46.
22. Whitnall M, Howard J, Ponka P, Richardson DR (2006) A class of iron chelators with a wide spectrum of potent antitumor activity that overcomes resistance to chemotherapeutics. Proc Natl Acad Sci U S A 103: 14901–14906.
23. Lovejoy DB, Sharp DM, Seebacher N, Obeidy P, Prichard T, et al. (2012) Novel second-generation di-2-pyridylketone thiosemicarbazones show synergism with standard chemotherapeutics and demonstrate potent activity against lung cancer xenografts after oral and intravenous administration in vivo. J Med Chem 55: 7230–7244.
24. Vitolo LMW, Hefter GT, Clare BW, Webb J (1990) Iron Chelators of the Pyridoxal Isonicotinoyl Hydrazone Class.2. Formation-Constants with Iron(Iii) and Iron(Ii). Inorganica Chimica Acta 170: 171–176.
25. Dubois JE, Fakhrayan H, Doucet JP, Chahine JME (1992) Kinetic and Thermodynamic Study of Complex-Formation between Iron(Ii) and Pyridoxal Isonicotinoylhydrazone and Other Synthetic Chelating-Agents. Inorganic Chemistry 31: 853–859.
26. Horackova M, Ponka P, Byczko Z (2000) The antioxidant effects of a novel iron chelator salicylaldehyde isonicotinoyl hydrazone in the prevention of H(2)O(2) injury in adult cardiomyocytes. Cardiovasc Res 47: 529–536.
27. Simunek T, Boer C, Bouwman RA, Vlasblom R, Versteilen AM, et al. (2005) SIH–a novel lipophilic iron chelator–protects H9c2 cardiomyoblasts from oxidative stress-induced mitochondrial injury and cell death. J Mol Cell Cardiol 39: 345–354.
28. Simunek T, Sterba M, Popelova O, Kaiserova H, Adamcova M, et al. (2008) Anthracycline toxicity to cardiomyocytes or cancer cells is differently affected by iron chelation with salicylaldehyde isonicotinoyl hydrazone. Br J Pharmacol 155: 138–148.
29. Berndt C, Kurz T, Selenius M, Fernandes AP, Edgren MR, et al. (2010) Chelation of lysosomal iron protects against ionizing radiation. Biochem J 432: 295–301.
30. Fillebeen C, Pantopoulos K (2010) Iron inhibits replication of infectious hepatitis C virus in permissive Huh7.5.1 cells. J Hepatol 53: 995–999.
31. Mackova E, Hruskova K, Bendova P, Vavrova A, Jansova H, et al. (2012) Methyl and ethyl ketone analogs of salicylaldehyde isonicotinoyl hydrazone: novel iron chelators with selective antiproliferative action. Chem Biol Interact 197: 69–79.
32. Klimtova I, Simunek T, Mazurova Y, Kaplanova J, Sterba M, et al. (2003) A study of potential toxic effects after repeated 10-week administration of a new iron chelator—salicylaldehyde isonicotinoyl hydrazone (SIH) to rabbits. Acta Medica (Hradec Kralove) 46: 163–170.
33. Hruskova K, Kovarikova P, Bendova P, Haskova P, Mackova E, et al. (2011) Synthesis and initial in vitro evaluations of novel antioxidant aroylhydrazone iron chelators with increased stability against plasma hydrolysis. Chem Res Toxicol 24: 290–302.
34. Richardson DR, Tran EH, Ponka P (1995) The potential of iron chelators of the pyridoxal isonicotinoyl hydrazone class as effective antiproliferative agents. Blood 86: 4295–4306.
35. Chaston TB, Lovejoy DB, Watts RN, Richardson DR (2003) Examination of the antiproliferative activity of iron chelators: multiple cellular targets and the different mechanism of action of triapine compared with desferrioxamine and the potent pyridoxal isonicotinoyl hydrazone analogue 311. Clin Cancer Res 9: 402–414.
36. Chaston TB, Richardson DR (2003) Redox chemistry and DNA interactions of the 2-pyridyl-carboxaldehyde isonicotinoyl hydrazone class of iron chelators: Implications for toxicity in the treatment of iron overload disease. J Biol Inorg Chem 8: 427–438.
37. Becker EM, Lovejoy DB, Greer JM, Watts R, Richardson DR (2003) Identification of the di-pyridyl ketone isonicotinoyl hydrazone (PKIH) analogues as potent iron chelators and anti-tumour agents. Br J Pharmacol 138: 819–830.
38. Richardson DR, Ponka P (1994) The iron metabolism of the human neuroblastoma cell: lack of relationship between the efficacy of iron chelation and the inhibition of DNA synthesis. J Lab Clin Med 124: 660–671.
39. Edward JT, Gauthier M, Chubb FL, Ponka P (1988) Synthesis of New Acylhydrazones as Iron-Chelating Compounds. Journal of Chemical and Engineering Data 33: 538–540.
40. Administration FaD (2001) Available: http://www.fda.gov/downloads/Drugs/GuidanceComplianceRegulatoryInformation/Guidances/UCM070107.pdf. Accessed 2014 September 15.
41. Kovarikova P, Mrkvickova Z, Klimes J (2008) Investigation of the stability of aromatic hydrazones in plasma and related biological material. J Pharm Biomed Anal 47: 360–370.
42. Esposito BP, Epsztejn S, Breuer W, Cabantchik ZI (2002) A review of fluorescence methods for assessing labile iron in cells and biological fluids. Anal Biochem 304: 1–18.
43. Glickstein H, El RB, Link G, Breuer W, Konijn AM, et al. (2006) Action of chelators in iron-loaded cardiac cells: Accessibility to intracellular labile iron and functional consequences. Blood 108: 3195–3203.
44. Richardson DR, Milnes K (1997) The potential of iron chelators of the pyridoxal isonicotinoyl hydrazone class as effective antiproliferative agents II: the mechanism of action of ligands derived from salicylaldehyde benzoyl hydrazone and 2-hydroxy-1-naphthylaldehyde benzoyl hydrazone. Blood 89: 3025–3038.
45. Baker E, Richardson D, Gross S, Ponka P (1992) Evaluation of the iron chelation potential of hydrazones of pyridoxal, salicylaldehyde and 2-hydroxy-1-naphthylaldehyde using the hepatocyte in culture. Hepatology 15: 492–501.
46. Richardson DR, Sharpe PC, Lovejoy DB, Senaratne D, Kalinowski DS, et al. (2006) Dipyridyl thiosemicarbazone chelators with potent and selective antitumor activity form iron complexes with redox activity. J Med Chem 49: 6510–6521.
47. Becker E, Richardson DR (1999) Development of novel aroylhydrazone ligands for iron chelation therapy: 2-pyridylcarboxaldehyde isonicotinoyl hydrazone analogs. J Lab Clin Med 134: 510–521.

48. Mladenka P, Kalinowski DS, Haskova P, Bobrovova Z, Hrdina R, et al. (2009) The novel iron chelator, 2-pyridylcarboxaldehyde 2-thiophenecarboxyl hydrazone, reduces catecholamine-mediated myocardial toxicity. Chem Res Toxicol 22: 208–217.
49. Chaston TB, Watts RN, Yuan J, Richardson DR (2004) Potent antitumor activity of novel iron chelators derived from di-2-pyridylketone isonicotinoyl hydrazone involves fenton-derived free radical generation. Clin Cancer Res 10: 7365–7374.
50. Repetto G, del Peso A, Zurita JL (2008) Neutral red uptake assay for the estimation of cell viability/cytotoxicity. Nat Protoc 3: 1125–1131.
51. Ghose AK, Crippen GM (1987) Atomic physicochemical parameters for three-dimensional-structure-directed quantitative structure-activity relationships. 2. Modeling dispersive and hydrophobic interactions. J Chem Inf Comput Sci 27: 21–35.
52. Viswanadhan VN, Ghose AK, Revankar GR, Robins RK (1989) Atomic physicochemical parameters for three dimensional structure directed quantitative structure-activity relationships. 4. Additional parameters for hydrophobic and dispersive interactions and their application for an automated superposition of certain naturally occurring nucleoside antibiotics. J Chem Inf Comput Sci 29: 163–172.
53. Broto P, Moreau G, Vandycke C (1984) Molecular Structures: Perception, Autocorrelation Descriptor and SAR Studies. System of Atomic Contributions for the Calculation of the *n*-Octanol/Water Partition Coefficients. Eur J Med Chem Chim Theor 19: 71–78.
54. Zhang XZ, Li M, Cui Y, Zhao J, Cui ZG, et al. (2012) Electrochemical Behavior of Calcein and the Interaction Between Calcein and DNA. Electroanalysis 24: 1878–1886.
55. Yuan J, Lovejoy DB, Richardson DR (2004) Novel di-2-pyridyl-derived iron chelators with marked and selective antitumor activity: in vitro and in vivo assessment. Blood 104: 1450–1458.
56. Gutteridge JM, Richmond R, Halliwell B (1979) Inhibition of the iron-catalysed formation of hydroxyl radicals from superoxide and of lipid peroxidation by desferrioxamine. Biochem J 184: 469–472.
57. Ponka P, Borova J, Neuwirt J, Fuchs O (1979) Mobilization of iron from reticulocytes. Identification of pyridoxal isonicotinoyl hydrazone as a new iron chelating agent. FEBS Lett 97: 317–321.
58. Kalia J, Raines RT (2008) Hydrolytic stability of hydrazones and oximes. Angew Chem Int Ed Engl 47: 7523–7526.
59. Kitazawa M, Iwasaki K (1999) Reduction of ultraviolet light-induced oxidative stress by amino acid-based iron chelators. Biochim Biophys Acta 1473: 400–408.
60. Bernhardt PV, Wilson GJ, Sharpe PC, Kalinowski DS, Richardson DR (2008) Tuning the antiproliferative activity of biologically active iron chelators: characterization of the coordination chemistry and biological efficacy of 2-acetylpyridine and 2-benzoylpyridine hydrazone ligands. J Biol Inorg Chem 13: 107–119.
61. Sies H (1993) Strategies of antioxidant defense. Eur J Biochem 215: 213–219.
62. Richardson D, Vitolo LW, Baker E, Webb J (1989) Pyridoxal isonicotinoyl hydrazone and analogues. Study of their stability in acidic, neutral and basic aqueous solutions by ultraviolet-visible spectrophotometry. Biol Met 2: 69–76.